REVISED DRAFT REPORT

GROUND MOTION RESPONSE SPECTRA, FOUR MILE PROJECT

Prepared for Quasar Resources Pty Ltd

Level 4, 25 Grenfell Street

Adelaide SA 5000

December 9, 2008

URS

566 El Dorado Street, 2nd Floor
Pasadena, California 91101

Table of Contents

EXECUTIVE SUMMARY

This report provides earthquake ground motion parameters for use in the design of the Four Mile mine. This site is located close to active faults of the Northern Flinders Ranges. Two categories of earthquake sources were used to represent the seismic hazard in the region. The first consists of active faults, and uses estimates of fault slip rate to quantify the seismic activity rate on the faults. The second earthquake source category consists of distributed seismicity.

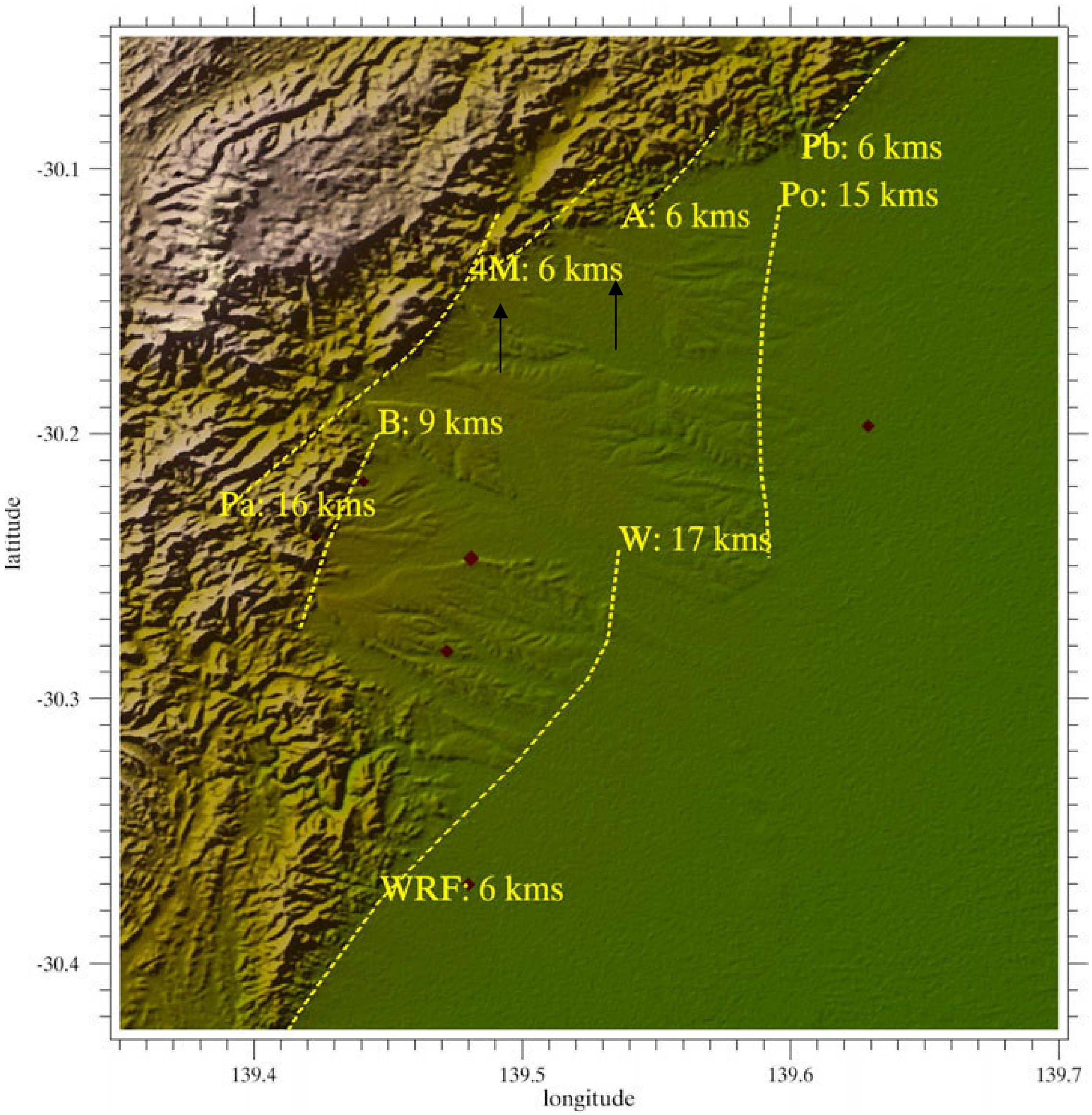

Figure E1. Faults in the Northern Flinders Ranges near Four Mile. The fault segments, clockwise from the west, are: B: Buxton; Pa: Paralana; 4M: Four Mile; A: Adams; Pb: Parabarana; Po: Poontana; W: Wooltana; and WRF: Wooltana Range Front. The Four Mile West and East sites are located at the heads of the two black arrows just east of the Four Mile Fault. Source: Sandiford (2008).

We commissioned a review by Mike Sandiford of active faults in the northeastern corner of the Northern Flinders Ranges (refer Attachment 1). He identified a system of four faults, shown in Figure E1, which include (clockwise from west) the Buxton, Paralana, Four Mile, Adams, Parabarana, Poontana, Wooltana, and Wooltana Range Front faults.

The Four Mile West and East sites are located at the heads of the two black arrows just east of the Four Mile Fault in Figure E1. These faults are all west-dipping reverse faults, and earthquakes on them cause the Flinders Ranges to rise in elevation above the adjacent Paralana High Plains. The Pontoona – Parabarana fault dips down to the west and underlies the Four Mile site. The site is 1.3 km east of the Paralana fault, but on the foot wall side because the Paralana fault also dips down to the west. Although the Four Mile mine site is located close to active faults, there is no indication that active faults intersect the Four Mile mine site.

Two alternative spatially distributed earthquake source models were used in this study. Both the AUS5 source model and the Risk Frontiers source model assume a maximum earthquake magnitude of Mw 7.5 throughout Australia. We consider that these models are equally viable alternative models of spatially distributed earthquake activity, so we use both of them in order to represent uncertainty in earthquake occurrence in the site region.

The Four Mile site is located within the tectonically active Flinders Ranges. We expect the ground motion characteristics at the site are intermediate between those for stable tectonic regions and those for more tectonically active regions. Accordingly, we have given equal weight to ground motion models that represent each of those two conditions..

As described by Heathgate (2008), the ground surface at the Four Mile site consists of about 15 metres of gravels of the Tertiary Willawortina formation, overlying the sands of the Tertiary Upper Eyre Formation. The mineralization occurs within the Tertiary Lower Eyre Formation at a depth ranging from 150 – 200 metres and averaging 180 metres.

In this report, we provide estimates of the ground motions at the surface and at 180 metres depth. In the ground motion models that we use, ground motion amplification in the near surfaces is estimated based on the average shear wave velocity in the top 30 metres of the soil profile (Vs30). We estimate that the Vs30 at the site is 400 metres/sec.

Several effects cause the ground motions at depth to be generally lower than those at the ground surface. We used data from downhole ground motion recordings at other locations to make very conservative estimates of the reduction factors at a depth of 180 metres. The surface ground motion levels were multiplied by a period dependent scaling factor ranging from 0.6 for peak acceleration and short periods to 0.9 for a period of 2 seconds.

The ground motion parameters are provided in the form of uniform hazard response spectra for a series of return periods ranging from 475 years to 10,000 years. The response spectra for the ground surface and for a depth of 180 metres below the ground surface at Four Mile West are shown in Figures E2 and E3 and listed in Tables E1 and E2. The ground motions at Four Mile East are slightly lower than those at Four Mile West.

The estimated peak acceleration values at the ground surface are listed in Table E3 for both Four Mile West and Four Mile East, for both ground surface level and a depth of 180 m below the ground surface. The peak acceleration values for return periods of 475, 1,000 and 10,000 years at the ground surface at Four Mile West, listed in Table E1, are 0.044g, 0.073g, and 0.374g respectively. The corresponding values at a depth of 180 metres below the ground surface, listed in Table E2, are 0.026g, 0.044g, and 0.224g respectively.

Table E1. Probabilistic Response Spectra (Sa in g's) at the ground surface at the Four Mile West Site for various Return Periods

Period	Sa at the Four Mile West Site for various ARP, g				
	475 yrs	1,000 yrs	3,000 yrs	5,000 yrs	10,000 yrs
0.00 sec (PGA)	0.044	0.073	0.163	0.236	0.374
0.05 sec	0.071	0.124	0.311	0.483	0.812
0.10 sec	0.085	0.144	0.324	0.467	0.729
0.15 sec	0.091	0.15	0.318	0.444	0.671
0.20 sec	0.094	0.151	0.305	0.416	0.619
0.25 sec	0.091	0.144	0.28	0.375	0.552
0.30 sec	0.088	0.137	0.259	0.344	0.503
0.40 sec	0.078	0.119	0.22	0.289	0.423
0.50 sec	0.067	0.103	0.185	0.242	0.355
0.75 sec	0.052	0.079	0.14	0.181	0.266
1.00 sec	0.045	0.068	0.121	0.157	0.227
1.50 sec	0.03	0.046	0.081	0.106	0.155
2.00 sec	0.023	0.035	0.062	0.08	0.117

Table E2. Probabilistic Response Spectra (Sa in g's) at a depth of 180 metres below the ground surface at the Four Mile West Site for various Return Periods

Period, sec	Reduction Factor	475 yrs	1,000 yrs	3,000 yrs	5,000 yrs	10,000 yrs
0.00 sec (PGA)	0.6000	0.0264	0.0438	0.0978	0.1416	0.2244
0.05 sec	0.6000	0.0426	0.0744	0.1866	0.2898	0.4872
0.10 sec	0.6000	0.0510	0.0864	0.1944	0.2802	0.4374
0.15 sec	0.6000	0.0546	0.0900	0.1908	0.2664	0.4026
0.20 sec	0.6000	0.0564	0.0906	0.1830	0.2496	0.3714
0.25 sec	0.6188	0.0563	0.0891	0.1733	0.2321	0.3416
0.30 sec	0.6375	0.0561	0.0873	0.1651	0.2193	0.3207
0.40 sec	0.6750	0.0527	0.0803	0.1485	0.1951	0.2855
0.50 sec	0.7125	0.0477	0.0734	0.1318	0.1724	0.2529
0.75 sec	0.8063	0.0419	0.0637	0.1129	0.1459	0.2145
1.00 sec	0.9000	0.0405	0.0612	0.1089	0.1413	0.2043
1.50 sec	0.9000	0.0270	0.0414	0.0729	0.0954	0.1395
2.00 sec	0.9000	0.0207	0.0315	0.0558	0.0720	0.1053

Table E3. Peak acceleration for various return periods.

Location	Peak Acceleration (g) at for various return periods				
	475 yrs	1,000 yrs	3,000 yrs	5,000 yrs	10,000 yrs
Four Mile West, ground surface	0.044	0.073	0.163	0.236	0.374
Four Mile East, ground surface	0.043	0.071	0.155	0.222	0.350
Four Mile West, -180 metres	0.026	0.044	0.098	0.142	0.224
Four Mile East, -180 metres	0.0258	0.0426	0.0930	0.1332	0.2100

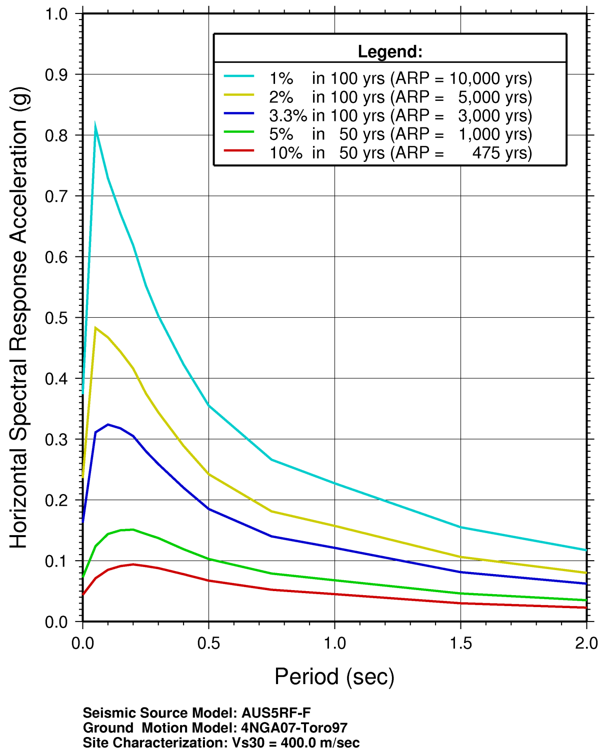

Figure E2. Probabilistic ground motion response spectra at the ground surface at Four Mile West for return periods of 475, 1,000, 3,000, 5,000 and 10,000 years.

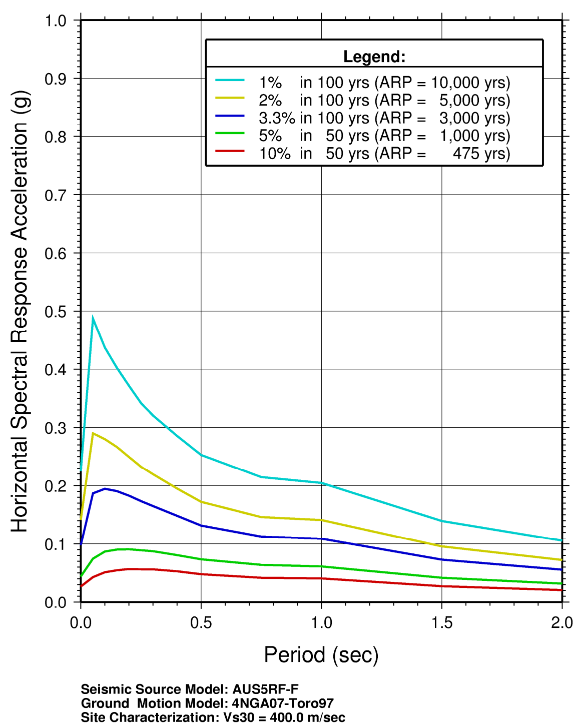

Figure E3. Probabilistic ground motion response spectra at a depth of 180 metres below the surface at Four Mile West for return periods of 475, 1,000, 3,000, 5,000 and 10,000 years.

1. INTRODUCTION

The objective of this report is to develop probabilistic ground motion response spectra at the Four Mile site for return periods of 475, 1000, 3000, 5000 and 10,000 years. The Four Mile site is shown in Figure 1.

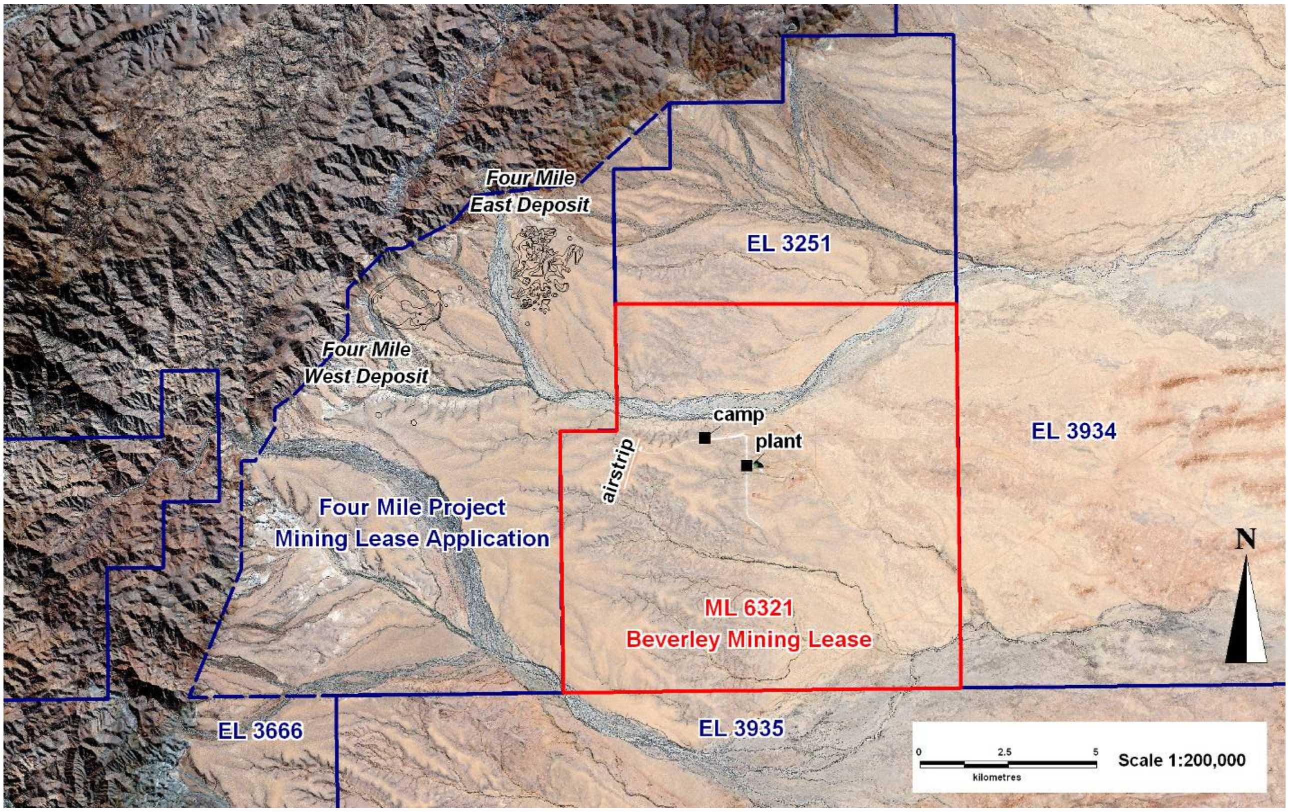

Figure 1. Location of the Four Mile East and Four Mile West sites.

Two categories of earthquake sources were used to represent the seismic hazard in the region. The first consists of active faults, and uses estimates of fault slip rate to quantify the seismic activity rate on the faults. We used newly available information from Quigley et al. (2006) and Sandiford (2008) to characterize these active faults.

The second earthquake source category consists of distributed seismicity. For this category, we used two alternative models. Each of these models was used in conjunction with the new active fault model. Throughout this report, we use moment magnitude Mw to describe the sizes of earthquakes, including those in historical catalogues as well as those used in earthquake recurrence models.

2. GEOLOGICAL SETTING AND ACTIVE FAULTS

2.1 Geological Setting

The Four Mile site is located in the Paralana High Plains, close to the eastern margin of the Flinders Ranges. The geological structure of the Four Mile site region is summarised in the stratigraphic cross-section of the Four Mile and Beverley areas shown in Figure 2. The orientation of the cross-section is approximately in a north-westerly direction from Beverley.

The region between the Poontana and Paralana faults is interpreted as a complex of fault-bounded blocks that are progressively higher to the west or north-west. The major basement relief on the cross section is caused by faulting but displacement magnitudes are difficult to establish. The Four Mile deposit is in an inferred NE trending half graben within the Paralana-Wertalonna structural zone. The Eyre Formation unconformably overlies Precambrian crystalline basement between the Poontana and Wooltana to the east and the Paralana fault to the west. These major faults are west-dipping structures that extend well down into Proterozoic basement rocks and show west over east compression.

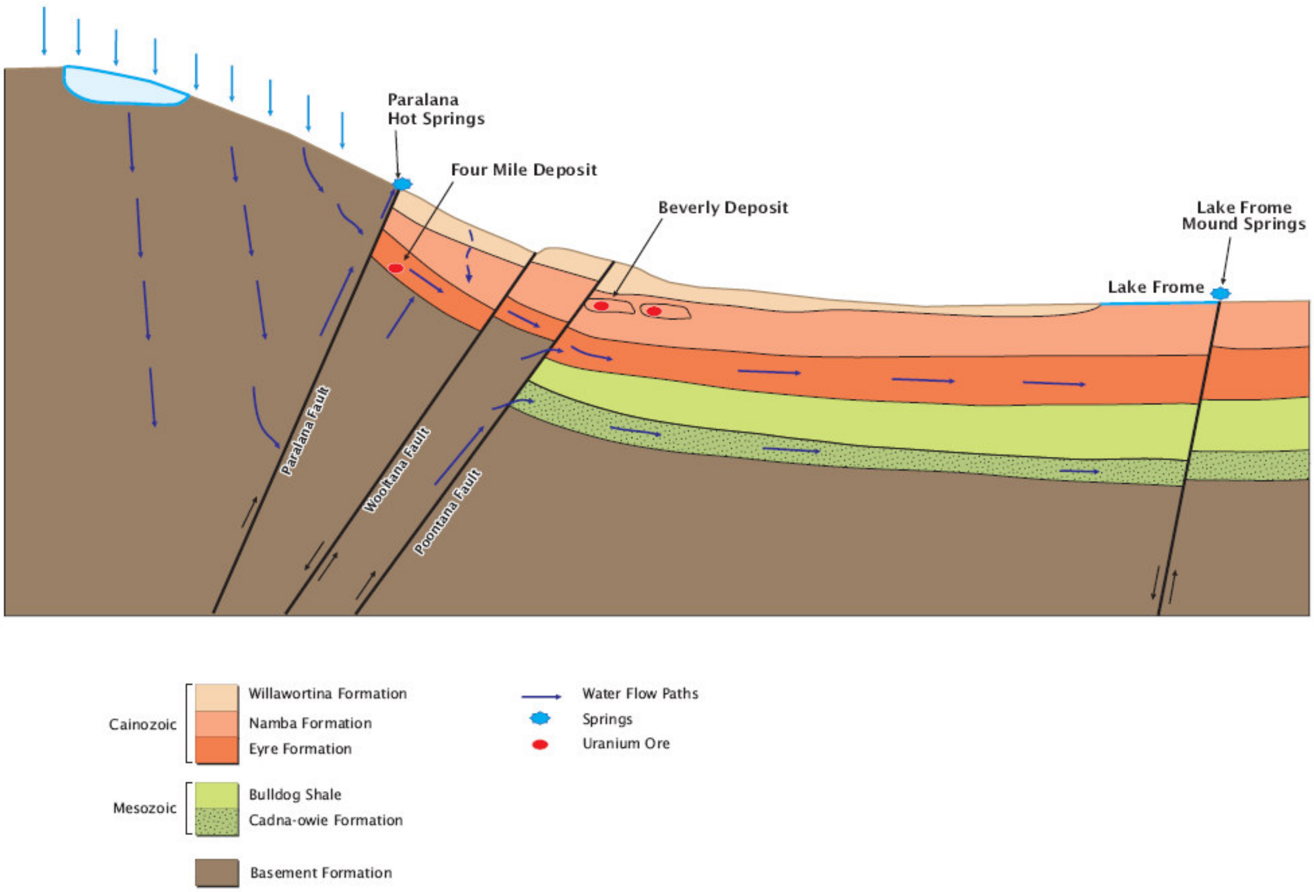

Figure 2. Geological cross section across the Four Mile site region. Source: Heathgate (2008).

2.2 Site Conditions for Ground Motion Estimation

For the purpose of selecting ground motion models that account for site effects, we need to characterize the shallow geology at the site. As described by Heathgate (2008), the ground surface at the Four Mile site consists of about 15 metres of gravels of the Tertiary Willawortina formation, overlying the sands of the Tertiary Upper Eyre Formation. The mineralization occurs within the Tertiary Lower Eyre Formation at a depth ranging from 150 – 200 metres and averaging 180 metres. In this report, we provide estimates of the ground motions at the surface and at 180 metres depth.

In the ground motion models that we use, ground motion amplification in the near surfaces is estimated based on the average shear wave velocity in the top 30 metres of the soil profile (Vs30). We are unaware of any measurements of shear wave velocity at the site, or of other measurements such as blow counts that could be used to estimate Vs30. Assuming an estimated Vs30 of 540 metres/sec for gravels and 290 metres/sec for sands (Borcherdt, 2004), we estimate that the Vs30 at the site is 400 metres/sec.

Several effects cause the ground motions at depth to be generally lower than those at the surface, so the ground motions at a depth of 180 metres are expected to be lower than those at the ground surface. We are unaware of any measurements at the site, such as shear wave velocities and parameters describing the reduction in shear modulus and increase in damping of the soils with increasing strain level, which would allow us to calculate the degree of reduction in ground motion level at a depth of 180 metres. We used reduction factors described in Section 5.3 based on downhole recordings of earthquake ground motions.

2.3 Active Faults

We commissioned a review by Mike Sandiford of active faults in the northeastern corner of the Northern Flinders Ranges (Sandiford, 2008; Attachment 1). He identified a system of four faults, shown in Figure 3, which include (clockwise from west) the Buxton, Paralana, Four Mile, Adams, Parabarana, Poontana, Wooltana, and Wooltana Range Front faults.

The Four Mile West and East sites are located at the heads of the two black arrows just east of the Four Mile Fault in Figure 3. These faults are all west-dipping reverse faults, and earthquakes on them cause the Flinders Ranges to rise in elevation above the adjacent Paralana High Plains.

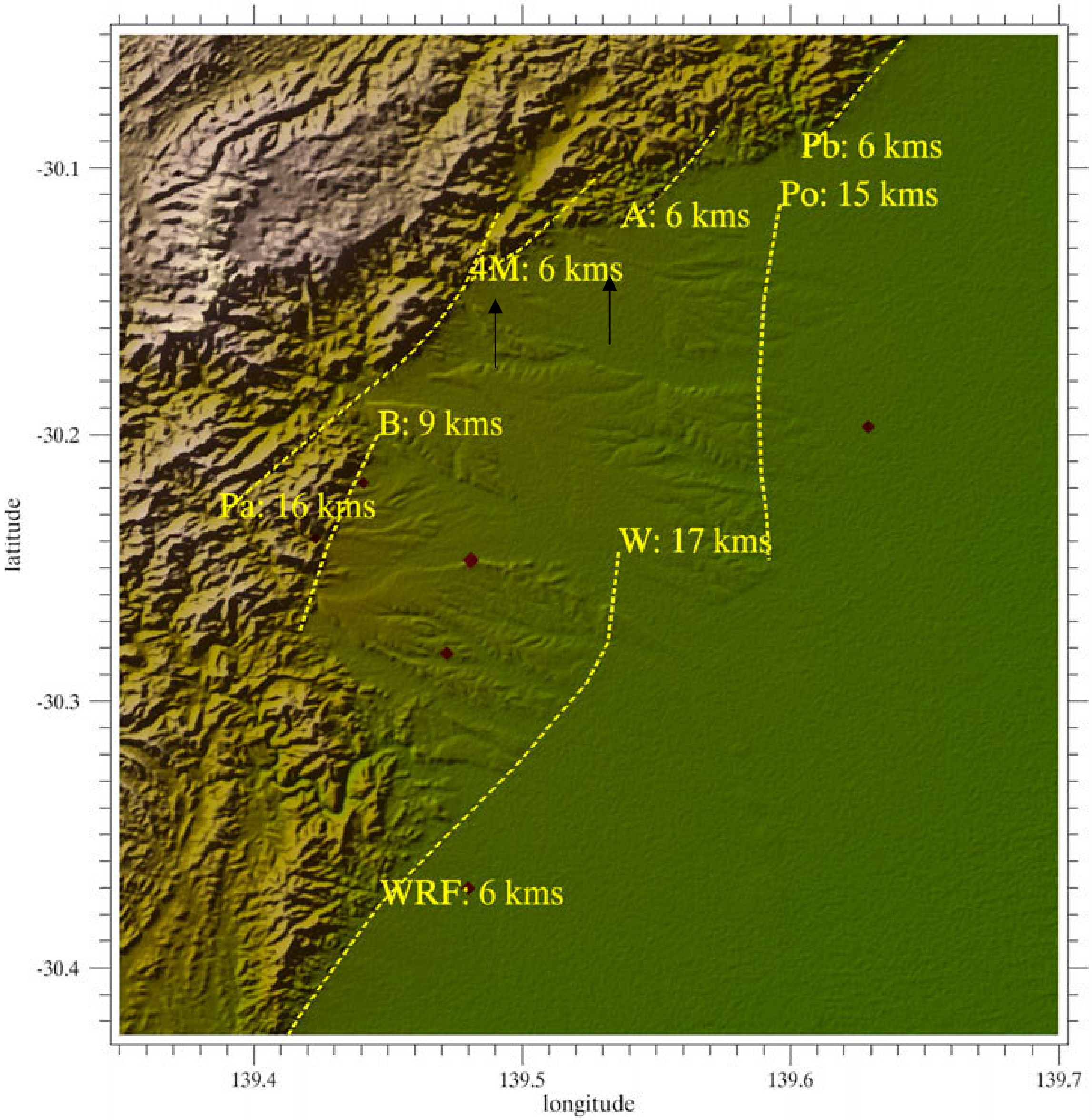

Figure 3. Faults in the Northern Flinders Ranges near Four Mile. The fault segments, clockwise from the west, are: B: Buxton; Pa: Paralana; 4M: Four Mile; A: Adams; Pb: Parabarana; Po: Poontana; W: Wooltana; and WRF: Wooltana Range Front. The Four Mile West and East sites are located at the heads of the two black arrows just east of the Four Mile Fault. Source: Sandiford (2008).

3. ACTIVE FAULT MODEL

For the purpose of seismic hazard modeling, we combined sets of faults because we consider that each set of faults has the potential to rupture in a single large earthquake, as well as to rupture as individual fault segments. These sets of faults, their estimated slip rates, and estimates of the magnitudes of the largest earthquakes that could occur on them are listed in Table 2.

The Buxton, Paralana, Four Mile, and Adams faults were combined into a single fault along the western margin of the range front. The Parabarana and Poontana faults were combined into a single fault along the northeastern margin of the range front. The Wooltana and Wooltana Range Front faults were combined into a single fault along the southwestern margin of the range front. The east-west offset between the Poontana and Wooltana faults is about 6 km, which is larger than the offset across which we consider it likely for a rupture to jump from one fault segment to another.

The fault parameters of the three faults are summarized in Table 2. The slip rates and dip angles of the faults are derived from the report by Sandiford (2008) in Attachment 1. The widths of the faults are based on the assumption that the seismicity in the Flinders ranges extends to about 20 km depth (Cummins et al., 2008, Figure 3). From these estimates of depth extent and dip angle, we have estimated the widths of the faults listed in Table 2.

Table 2. Active Fault Parameters

Scenario Segments	**Length**	**Dip**	**Width***	**Area**	**Mmax**	**R#**	**Slip Rate,** median + range
Buxton + Paralana + Four Mile + Adams	29	40	31.1	902	7.20	1.3	0.03 mm/yr; 0.01 – 0.05 mm/yr
Pontoona + Parabarana	24	25	47.3	1143	7.31	0.0	0.065 mm/yr; 0.03 – 0.1 mm/yr
Wooltana + W. Range Front	23	25	47.3	1095	7.29	10.0	0.03 mm/yr; 0.01 – 0.05 mm/yr

*Assumes that the seismogenic zone extends from the surface to 20 km depth
Joyner-Boore distance from Four Mile West site

In estimating the maximum magnitudes of the earthquakes listed in Table 2, we used the relationship between rupture area and earthquake magnitude derived for Central and Western Australian earthquakes derived by Somerville. (2008), based on rupture model inversions of the 1968 Meckering and 1988 Tennant Creek earthquakes. This relationship is:

$$Mw = \log10\ A + 4.25.$$

Ranges of slip rates on the faults are given by Sandiford (2008) in Attachment 1. To represent uncertainty in the slip rate for the Pontoona – Parabarana fault, we used a distribution of values, giving a weight of 0.6 to the median value of 0.065 mm/year, and weights of 0.2 to values of 0.03 mm/year and 0.1 mm/year. To represent uncertainty in the slip rate for the Buxton - Paralana – Four Mile - Adams fault, and for the Wooltana – Wooltana Range Front fault, we similarly used a distribution of values, giving a weight of 0.6 to the median value of 0.03 mm/year, and weights of 0.2 to values of 0.01 mm/year and 0.05 mm/year.

The distances between the faults and the Four Mile West site are shown in Table 2. These distances use the Joyner-Boore definition (Abrahamson and Shedlock, 1997), which measures the closest distance from the site to the vertical surface projection of the fault plane. This distance definition is used in the ground motion models described below.

According to this definition, all sites on the hanging wall of a fault are at zero distance. This is the case for the Pontoona – Parabarana fault because it dips down to the west and underlies the Four Mile site. The site is 1.3 km east of the Paralana fault, but on the foot wall side because the Paralana fault also dips down to the west, so its Joyner-Boore distance is 1.3 km.

3.1 Distributed Earthquake Sources

While it is usually possible to associate large historical earthquakes with known active faults, especially if the faults break the ground surface, it is generally the case that small earthquakes can occur in places where active faults have not been identified. Thus we need to consider distributed earthquake sources in addition to the active faults described above.

In the following sections, we describe the historical seismicity of the site region, and then describe two distributed earthquake models that have been derived from seismicity and other data. These are the AUS5 (2001) and the Risk Frontiers (2007) models, and we consider that they are equally viable alternative models of spatially distributed earthquake activity, so we use both of them in order to represent uncertainty in how that seismicity occurs in the region. We use the active fault model described in Table 2 in conjunction with both of the distributed earthquake source models described in the following sections.

4. HISTORICAL SEISMICITY

Earthquake epicentres in the northeastern Flinders Ranges region are shown in Figure 4, and all known earthquakes within 80 km of Four Mile are listed in order of epicentral distance in Attachment 2. The uncertainty in each location is normally between ±5 and ±20 km in longitude and latitude. Many of the depths are very poorly constrained. The largest event within 80 km is only of magnitude ML 4.0 (2005-03-03 at distance 78 km), and most of the listed events have magnitude less than ML 2.0.

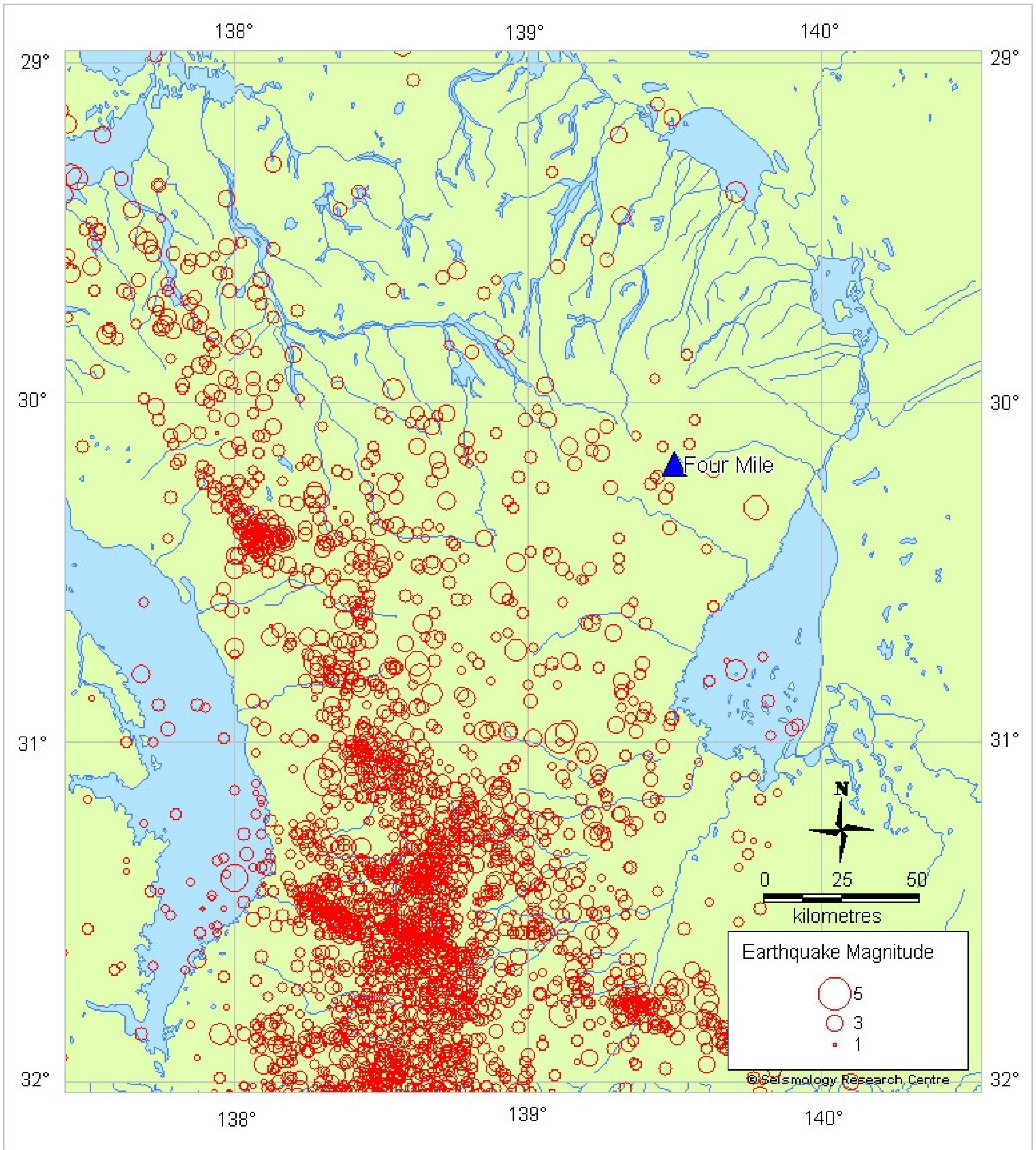

Figure 4. Historical seismicity, including aftershocks, of the Northern Flinders Ranges region. Source: Gibson (2008).

4.1 Estimated Earthquake Intensities at Four Mile

Table 3 lists the estimated intensities of known earthquakes at the Four Mile sites. The list includes both small nearby events, and large distant events, including the 1941-06-27 Simpson Desert Ms 6.5 event. It includes all events that would give an estimated Modified Mercalli intensity of 2 or greater at Four Mile, computed using the simple Esteva & Rosenblueth 1964 function.

Table 3: Estimated intensities of earthquakes at the Four Mile site

Srce	Time		Lon E	Lat S	Depth		Mag	dist	PGA	MM	Location
ADE	1971-11-05	1611	139.8	30.3	7		ML 3.7	31	278.1	4	Paralana
ADE	1939-03-26	0356	138.3	31.1	0		Ms 5.7	154	79.6	3	Parachilna
ADE	1990-02-11	0937	139.5	30.3	7		ML 2.3	12	217.2	3	Arkaroola
ISC	1965-03-02	1518	138.4	30.6	33	N	ML 5.0	116	73.1	3	Leigh Creek
ISC	1983-12-29	1741	138.3	30.8	20	G	mb 5.1	133	64.4	3	Beltana
ADE	1984-09-22	0052	139.3	30.2	1		ML 2.6	24	161.7	3	Umberatana Stn
ADE	1989-01-06	1305	139.6	30.2	2	G	ML 2.1	13	191.0	3	Arkaroola
ADE	2005-05-14	1953	139.1	31.0	20		ML 4.5	97	71.7	3	Mt Chambers
ADE	1972-04-18	2220	138.6	31.6	12		ML 5.4	176	47.5	3	Wilpena Pound
ISC	2005-03-03	1056	139.1	30.8	10		ML 4.0	78	75.0	3	Mulga View HS
ADE	1998-10-13	1009	139.4	30.2	12		ML 2.0	7	164.1	2	Arkaroola
EIDC	1996-11-09	1126	139.1	30.1	0		ML 2.8	35	115.0	2	Umberatana
ADE	1988-02-10	2000	139.4	30.2	0		ML 1.8	10	169.6	2	Arkaroola
ADE	1971-07-26	0750	138.8	31.4	19		ML 4.9	150	43.2	2	Brachina
ADE	1979-02-22	0925	139.5	30.4	17		ML 2.3	21	114.9	2	Arkaroola
ADE	1983-06-15	2314	139.3	30.1	11		ML 2.3	26	105.4	2	Mt Freeling
ADE	1990-02-10	2209	139.5	30.2	3		ML 1.5	8	142.7	2	Arkaroola
ADE	1987-07-12	0119	139.3	30.2	5		ML 2.0	22	108.7	2	Arkaroola
ISC	1965-03-14	1247	138.5	32.0	26	G	mb 5.3	216	29.0	2	Hawker
ADE	1982-12-22	1645	139.6	30.1	0		ML 1.7	16	120.3	2	Mt Fitton
ADE	1993-06-24	1302	139.5	30.1	11		ML 1.6	7	124.0	2	Arkaroola
ADE	2004-01-19	0754	139.4	30.2	10		ML 1.5	8	120.0	2	Arkaroola
ADE	1994-07-08	1840	138.9	30.6	14		ML 3.3	70	50.9	2	Nepabunna
ADE	1959-05-21	1128	139.0	31.4	10	N	ML 4.4	143	32.1	2	Martins Well HS
BMR	1941-06-27	0755	137.3	26.0	0	R	Ms 6.5	514	13.7	2	Simpson Desert
ADE	1986-12-16	0712	139.2	30.1	0		ML 2.0	28	82.6	2	Umberatana
ADE	1969-03-04	0419	139.0	30.7	2		ML 3.4	80	44.9	2	Nepabunna

This function overestimates intensities in eastern Australia a little, and probably slightly underestimates intensities in the older, harder rock of South Australia. Intensity MM 8 damages engineered structures that are well-designed and built, MM 6 damages normal buildings, and MM 4 is felt by most people, MM 3 by many people, and MM 2 by few people.

The strongest motion at Four Mile from a known earthquake is only MM 4, from a small local event in 1971, and only 10 events give intensity of 3 or greater. This compares with estimates computed using the same method in the Eastern Highlands between Melbourne and Newcastle, where the maximum estimated intensity is typically about MM 6, and there are often 100 or more events giving an estimated intensity of MM 3 or higher.

This shows that historically, the hazard has been lower in the Four Mile site region than in the Eastern Highlands, but over longer periods of time, the active faults near Four Mile have the potential to generate large intensities at the Four Mile site.

5. SPATIALLY DISTRIBUTED EARTHQUAKE SOURCE MODELS

Two alternative spatially distributed earthquake source models were used in this study. Both the AUS5 source model and the Risk Frontiers source model assume a maximum earthquake magnitude of Mw 7.5 throughout Australia. We consider that the AUS5 (2001) and the Risk Frontiers (2007) models are equally viable alternative models of spatially distributed earthquake activity, so we use both of them in order to represent uncertainty in earthquake occurrence in the site region.

5.1 AUS5 Earthquake Source Model

The first is the AUS5 source model used by SRC (2001). This model is based on the approach of Brown and Gibson (2000, 2004), which uses geological criteria to identify zones of uniform seismic potential, and then uses historical seismicity to characterize the seismic potential of each zone by means of the a-values and b-values of the Gutenberg-Richter earthquake recurrence model, described in Attachment 2, together with an estimate of the maximum magnitude of earthquakes in each zone. The zones in the site region are shown in Figure 5, and the a-values and b-values of these zones are listed in Table 4.

Table 4. AUS5 model a-values and b-values

Source Zone	A0	b	a	N(M=5)	R*
Broken Hill	42.024	0.939	1.62349739	0.00084820	207
Cobar	11.000	0.800	1.04139269	0.00110000	311
Coorong	10.650	0.880	1.02734961	0.00042398	555
Denison	196.860	0.993	2.29415748	0.00213382	3
Eromanga	3.300	0.800	0.51851394	0.00033000	187
Flinders Ranges	703.700	0.952	2.84738755	0.01218674	139
Gawler	6.000	0.880	0.77815125	0.00023886	291
Grampians	28.000	0.780	1.44715803	0.00352499	791
Kangaroo Island	33.000	0.880	1.51851394	0.00131375	609
Kanmantoo	95.000	0.880	1.97772361	0.00378202	457
Leigh Creek	567.390	0.963	2.75388168	0.00868724	95
Murray Darling	4.000	0.780	0.60205999	0.00050357	359
Murray Shelf	13.060	0.780	1.11594318	0.00164416	607
Otway Basin	6.200	0.850	0.79239169	0.00034865	725
Otway Shelf	7.000	0.850	0.84509804	0.00039364	819
Renmark	10.980	0.880	1.04060234	0.00043712	291
Spencer Gulf	26.000	0.880	1.41497335	0.00103508	335
Stuart Shelf	17.410	0.980	1.24079877	0.00021918	153
Warburton Basin	4.150	0.724	0.61804810	0.00099094	13
Whyalla	93.380	0.809	1.97025387	0.00841887	297
Wimmera	30.000	0.780	1.47712125	0.00377678	647

* R = Joyner-Boore distance between source and Four Mile West (km)

The AUS5 model assumes that earthquake activity depends on the interaction between of the geological structure and the stress field, and that variations in seismogenic upper crustal geology (not the surface geology) are the cause of variations in seismicity on a scale to tens or hundreds of kilometres, with variations in the stress field on this scale correlating with these geological variations, while stress variations on a larger scale depend on large scale global tectonics. The AUS5 model sometimes incorporates broad regional seismicity variations (that presumably result from large scale stress field variations) by including several area zones, with relatively minor variations from one zone to the next.

The seismotectonic model was initially drawn with zonation based on regional geology and geophysics throughout Australia. There has been much iteration in the model since the first AUS1 version was developed, especially in areas where detailed seismic hazard studies have been conducted in Victoria and eastern New South Wales. In other areas, such as the remote regions of South Australia including the North Flinders Ranges area, the original zonation remains undeveloped.

A problem associated with seismicity studies in South Australia is the large number of large blasts, mainly associated with coal mining near Leigh Creek, or mining in the Olympic Dam area. Many large blasts have been included as earthquakes in the catalogues, and international earthquake catalogues from the IDC, USGS and ISC contain these.

However, as a further complication, once an area has been identified as a source of large blasts, it is common to assume that all events from that region are blasts, whereas it is possible that some of these are earthquakes. Some large coal mines now provide routine mine safety blast information emails to seismograph authorities to help distinguish blasts from earthquakes.

5.2 RF Earthquake Source Model

The second earthquake source model was derived by Risk Frontiers (Hall et al., 2007) based on the spatial smoothing of historical seismicity, and is described further in Attachment 2. This approach is similar to the main approach used to describe the seismic potential of the eastern United States in the U.S. National Probabilistic Seismic Hazard Maps (Frankel et al., 2007).

This spatially distributed earthquake source model was derived from the spatial smoothing of historical seismicity using the earthquake catalogue described by Leonard (2006). It is intended that this model complement other models, such as Brown and Gibson (2004) and Ninis and Gibson (2006), which use geological criteria to identify zones of uniform seismic potential, and Clark (2006), which uses neotectonic data.

The spatial smoothing approach has the advantages of simplicity and of avoiding uncertainty in the geological definitions of zones, but has the disadvantage of not making use of potentially informative geological data. The spatially distributed earthquake source model is in the form of a-values and b-values on a 10 km x 10 km grid throughout Australia.

The b-values for each of the five zones in Leonard (2006) were generated using completeness intervals listed in Attachment 2, Table A3.1: Southeastern Australia (SEA), Southwestern Australia (SWA), South Australia (SA), Northwestern Australia (NWA), and the rest of Australia. The a-value grids for each region were derived from the smoothed spatial distribution of seismicity, using the b-value for that zone and the number of earthquakes greater than or equal to a certain magnitude within each grid cell. We used three lower magnitude cutoff values: M3, M4 and M5, and averaged the results. Separate a-value grids were calculated for each zone.

For each a-value grid point, the number of events ≥ M0 was calculated, and the grids for each region were summed to give country-wide coverage of the number events ≥ M0. Kernel density algorithms were used to calculate smoothed seismicity density for each input data set.

In regions with longer completeness intervals and hence higher densities of events (SEA, SWA, SA and NWA), a correlation distance of 100 km was applied. Further details of the Risk Frontiers model are described in Attachment 3. The Four Mile site is located within the South Australia zone. The rate of occurrence of earthquakes having magnitude 5 in the Risk Frontiers distributed earthquake source model is shown in Figure 6.

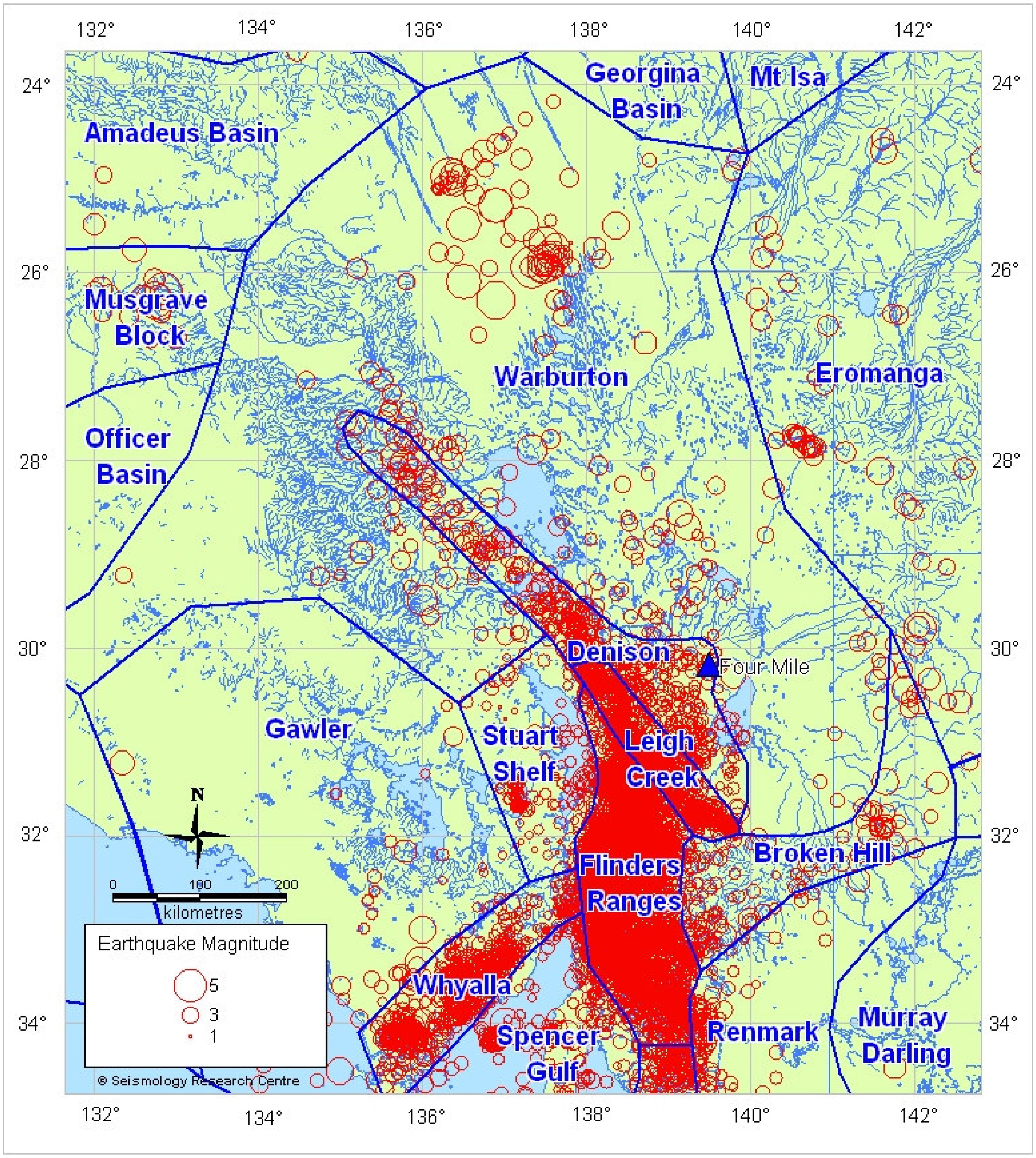

Figure 5. Source Zones of the updated AUS5 Earthquake Source Model. Aftershocks are shown but are excluded from the source zone models. Source: Gibson (2008)

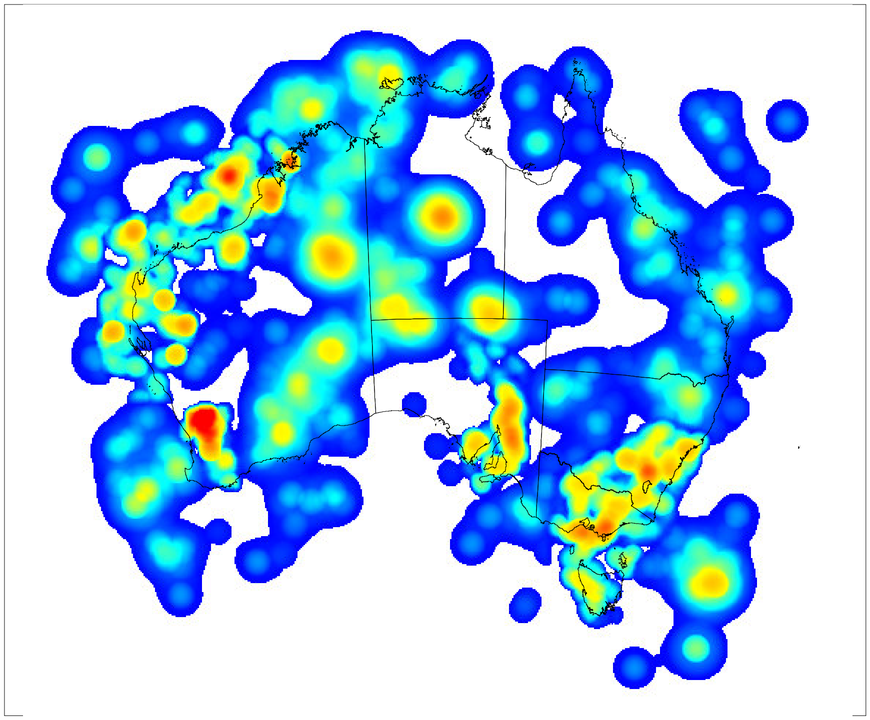

Figure 6. Grid of number of events of M>5 per 500 years per 10,000 square km in the RF source model. Source: Hall et al. (2007).

6. GROUND MOTION MODELS

The objective of this section is to select models that are appropriate for the prediction of strong ground motions at Four Mile.

6.1 Review of Australian Ground Motion Models and Data

In recent years, considerable work has been devoted to characterizing earthquake ground motions in Australia for use in seismic hazard analyses. To date, no response spectral ground motion models have been developed for Australia. Accordingly, we have selected ground motion models from other regions that are considered to be potentially applicable in Australia.

Recent earthquake hazard and risk assessments in Australia by Geoscience Australia have typically adopted ground motion models from other stable continental regions such as eastern North America (ENA), in particular Toro et al. (1997). However, it has been suggested that ENA attenuation is extremely low, and stable continental regions such as Australia and India lie somewhere between the eastern and western U.S. (Bakun and McGarr, 2002). Further, it appears that differences in attenuation may exist between the eastern and western parts of Australia due to variations in crustal properties. The western part of Australia is an Archean craton, while the eastern part consists of Palaeozoic crust.

Brown and Gibson (2004) analyzed the attenuation of recorded ground motion in eastern Australia from three earthquakes in the magnitude range of 4.8 to 5.1 in eastern New South Wales and Victoria (Figure 9 of their paper), and showed that it is more compatible with the Sadigh et al. (1997) model than the Toro et al. (1997) model.

Recent work by Allen et al. (2005) and McPherson and Allen (2006) using stochastic modeling of ground motions in Southeastern Australia also produces response spectra whose shapes are more compatible with the Sadigh et al. (1997) model than the Toro et al. (1997) model.

Allen et al. (2005) and McPherson and Allen (2006) analyzed the attenuation of vertical component ground motions in 1200 strong motion and weak motion recordings from 87 earthquakes in southeastern New South Wales and Victoria ranging in magnitude from 2.0 to 4.7. Many of the recordings came from Environmental Systems and Services (ES&S) and the study was sponsored in part by the Australian Committee on Large Dams (ANCOLD). These studies conclude that ground motions attenuate more rapidly in southeastern Australia that in ENA.

Allen and Atkinson (2006) present a comparison between spectral amplitude databases from small-to-moderate events (moment magnitudes $2.0 \leq M \leq 5.0$) in both southeastern Australia (SEA) and eastern North America. Source and attenuation properties of the two regions are found to be similar, particularly at shorter hypocentral distances R (i.e. $R < 70$ km) and frequencies < 10 Hz. At larger distances, ground motions attenuate more rapidly in southeastern Australia that in ENA.

The Four Mile site is located within the tectonically active Flinders Ranges. We expect the ground motion characteristics at the site are intermediate between those for the WUS and ENA. Accordingly, we have given them equal weight. The four NGA models for the WUS, described further below, were each given the same weight (0.125), or a total weight of 0.5, and the Toro et al. (1997) model was given a weight of 0.5.

6.2 Selection of Ground Motion Models

We reviewed available ground motion models for crustal earthquakes in tectonically stable regions. These include Toro *et al.,* (1997), Frankel *et al.,* (1995), Atkinson and Boore (1995, 2005), Campbell (2003), and Somerville *et al.,* (2001).

We conclude that the Toro et al. (1997) is the most broadly based and completely documented model available, and have chosen it to represent the possibility that the ground motions at the site have characteristics like those in stable continental regions. This model mainly represents the ground motions of reverse faults, and is therefore appropriate for use in eastern Australia where the predominant earthquake mechanism is thought to be reverse.

The Toro et al. (1997) model is for a surface shear wave velocity (Vs30) of 2.84 km/sec. To adjust this to the surface shear wave velocity of about 0.4 km/sec at the Four Mile site, we increase the Toro et al. (1997) ground motion values by period dependent factors. These amplification factors, listed in Table 5, are derived from the 2002 NEHRP amplification factors.

Using the NEHRP factors, we represent Vs30 of 400 m/sec by the boundary between NEHRP sites C and D, and Vs 2.84 km/sec by NEHRP site A. This is judged to be a conservative representation of factors that would be obtained using a more rigorous approach. The five selected ground motion models and their weights are listed in Table 5.

Table 5. Ground Motion Models and Weights

Model	Vs30 (km/sec)	Tectonic Environment	Weight
Abrahamson and Silva (2007)	0.4	Active (global)	12.5%
Boore and Atkinson (2007)	0.4	Active (global)	12.5%
Campbell and Bozorgnia (2007)	0.4	Active (global)	12.5%
Chiou and Youngs (2007)	0.4	Active (global)	12.5%
Toro et al. (1997)	2.84; scale up by factor to adjust*	Stable (ENA)	50%

* Factor = 2.56 for T = 2.0 and 1 sec; 1.95 for T = 0.4 sec, and 1.75 for T = 0.2 sec and less

We reviewed available ground motion models for crustal earthquakes in tectonically active regions. These include the recently developed NGA ground motion models. NGA response spectral models were developed by five groups: Abrahamson and Silva (2008), Boore and Atkinson (2008); Campbell and Bozorgnia (2008), Chiou and Youngs (2008), and Idriss (2008).

In view of the great care that was put into documenting the NGA metadata that describe the strong motion recordings, the vastly larger size of the data set that has been used, and the diligence that has been applied by the modelers, we conclude that the NGA Program has resulted in a set of ground motion models that have a much more substantial basis than the 1997 generation of models.

In particular, the specification of site response using Vs30 has provided much greater flexibility in the application of these models to hard rock sites. Although recordings from such sites are still poorly represented in these new models, it is judged that they can be reliably extrapolated to Vs30 values as high as 2 km/sec.

We have given equal weights to the first four NGA models, and do not use the Idriss (2007) model because is not available for soil site conditions. The NGA models supersede the previous set of models developed by essentially the same set of investigators that were published in 1997 (Boore *et al.*, 1997; Sadigh *et al.,* 1997; Abrahamson and Silva, 1997) or subsequently modified (Campbell and Bozorgnia, 2003).

6.3 Ground Motions at Depth

Our objective is to estimate ground motion levels at depth as well as at the ground surface at Four Mile. Several effects cause the ground motions at depth to be generally lower than those at the surface.

First, the effect of the free surface of a homogeneous medium is approximately to double the amplitude of the incident wave over a depth that increases with the period of the wave. Second, the general gradient of increasing shear wave velocity and density with depth causes amplification of the ground motion in addition to that due to the free surface effect.

Accordingly, the ground motions at a depth of 180 metres are expected to be lower than those at the ground surface. We are unaware of any measurements at the site, such as shear wave velocities and parameters describing the reduction in shear modulus and increase in damping of the soils with increasing strain level, which would allow us to calculate the degree of reduction in ground motion level at a depth of 180 metres.

We used data from downhole ground motion recordings to make very conservative estimates of the reduction factors at a depth of 180 metres. Examples of such data are given in Hu and Xie (2004). These factors are listed in Tables 8 and 9. It is likely that site-specific soil data would lead to the calculation of significantly larger reductions.

7. PROBABILISTIC SEISMIC HAZARD ANALYSIS

7.1 Methodology

The Probabilistic Seismic Hazard Analysis (PSHA) is based on methodology originally proposed by Cornell (1968) and we will present a brief overview of the method as well as specific information on the parameters and models used in our analysis. If seismicity is considered to follow a random Poisson process, as we have assumed here, then the probability that a ground motion, such as Spectral Acceleration (SA) exceeds a certain value (s) in a time period t is given by:

$$P(SA > s) = 1 - e^{-\phi(s)t}$$

where $\phi(s)$ is the annual mean number of events (also known as "annual frequency of exceedance") in which the ground motion parameter of interest exceeds the value *s*.

For engineering purposes, we are interested in computing s for a certain probability of occurrence, P, in a time period t. For this project, the targets are annual frequencies of exceedance of 1/475, and 1/1000, 1/3000, 1/5000 and 1/10000 respectively. We usually refer to the latter in terms of return period, i.e. 475, 1000, 3000, 5000 and 10000 years respectively.

The annual frequency of exceedance is calculated as follows:

$$\phi(s) = \sum_{i=1}^{Faults} \left(\iint_{m,r} f(m)(P(SA > s \mid m,r)P(r \mid m)dmdr\right)_i$$

where:

$f(m_i)$ = probability density function for events of magnitude m_i

$P(SA>s|m,r)$ = probability that *SA* exceeds *s* given magnitude *m* and distance *r*

$P(r|m)$ = probability that the source to site distance is *r*, given a source of magnitude *m*.

The probabilistic analysis was performed using the program developed by Abrahamson (pers. comm., 2002). The random variability in all of the ground motion models was truncated at 3 standard deviations above the median value.

7.2 Equal Hazard Response Spectra

Probabilistic seismic hazard calculations were done for two sites: Four Mile East and Four Mile West. The Four Mile West site is closer to the Paralana fault and for that reason has higher ground motion levels. The response spectra for return periods of 475, 1,000, 3,000, 5,000 and 10,000 years for 5% of critical damping at the ground surface are shown in Figures 7 and 8 for the two sites, and are also tabulated in Tables 6 and 7.

The corresponding results for a depth of 180 metres below the ground surface are shown in Figures 9 and 10 and Tables 8 and 9. The peak acceleration (PGA) values are equivalent to the zero period values.

Table 6. Probabilistic Response Spectra (Sa in g's) at the ground surface at the Four Mile West Site for various Return Periods

Period	Sa at the Four Mile West Site for various ARP, g				
	475 yrs	1,000 yrs	3,000 yrs	5,000 yrs	10,000 yrs
0.00 sec (PGA)	0.044	0.073	0.163	0.236	0.374
0.05 sec	0.071	0.124	0.311	0.483	0.812
0.10 sec	0.085	0.144	0.324	0.467	0.729
0.15 sec	0.091	0.15	0.318	0.444	0.671
0.20 sec	0.094	0.151	0.305	0.416	0.619
0.25 sec	0.091	0.144	0.28	0.375	0.552
0.30 sec	0.088	0.137	0.259	0.344	0.503
0.40 sec	0.078	0.119	0.22	0.289	0.423
0.50 sec	0.067	0.103	0.185	0.242	0.355
0.75 sec	0.052	0.079	0.14	0.181	0.266
1.00 sec	0.045	0.068	0.121	0.157	0.227
1.50 sec	0.03	0.046	0.081	0.106	0.155
2.00 sec	0.023	0.035	0.062	0.08	0.117

Table 7. Probabilistic Response Spectra (Sa in g's) at the ground surface at the Four Mile East Site for various Return Periods

Period	Sa at the Four Mile East Site for various ARP, g				
	475 yrs	1,000 yrs	3,000 yrs	5,000 yrs	10,000 yrs
0.00 sec (PGA)	0.043	0.071	0.155	0.222	0.350
0.05 sec	0.069	0.121	0.294	0.446	0.749
0.10 sec	0.083	0.140	0.307	0.438	0.683
0.15 sec	0.089	0.146	0.303	0.420	0.635
0.20 sec	0.092	0.147	0.292	0.396	0.588
0.25 sec	0.090	0.141	0.269	0.359	0.528
0.30 sec	0.087	0.134	0.250	0.331	0.482
0.40 sec	0.077	0.117	0.213	0.279	0.406
0.50 sec	0.066	0.101	0.179	0.235	0.342
0.75 sec	0.052	0.078	0.136	0.177	0.257
1.00 sec	0.045	0.067	0.118	0.153	0.220
1.50 sec	0.030	0.046	0.080	0.104	0.151
2.00 sec	0.023	0.035	0.061	0.079	0.114

Table 8. Probabilistic Response Spectra (Sa in g's) at a depth of 180 metres below the ground surface at the Four Mile West Site for various Return Periods

Period, sec	Reduction Factor	475 yrs	1,000 yrs	3,000 yrs	5,000 yrs	10,000 yrs
0.00 sec (PGA)	0.6000	0.0264	0.0438	0.0978	0.1416	0.2244
0.05 sec	0.6000	0.0426	0.0744	0.1866	0.2898	0.4872
0.10 sec	0.6000	0.0510	0.0864	0.1944	0.2802	0.4374
0.15 sec	0.6000	0.0546	0.0900	0.1908	0.2664	0.4026
0.20 sec	0.6000	0.0564	0.0906	0.1830	0.2496	0.3714
0.25 sec	0.6188	0.0563	0.0891	0.1733	0.2321	0.3416
0.30 sec	0.6375	0.0561	0.0873	0.1651	0.2193	0.3207
0.40 sec	0.6750	0.0527	0.0803	0.1485	0.1951	0.2855
0.50 sec	0.7125	0.0477	0.0734	0.1318	0.1724	0.2529
0.75 sec	0.8063	0.0419	0.0637	0.1129	0.1459	0.2145
1.00 sec	0.9000	0.0405	0.0612	0.1089	0.1413	0.2043
1.50 sec	0.9000	0.0270	0.0414	0.0729	0.0954	0.1395
2.00 sec	0.9000	0.0207	0.0315	0.0558	0.0720	0.1053

Table 9. Probabilistic Response Spectra (Sa in g's) at a depth of 180 metres at the Four Mile East Site for various Return Periods

Period, sec	Reduction Factor	475 yrs	1,000 yrs	3,000 yrs	5,000 yrs	10,000 yrs
0.00 sec (PGA)	0.6000	0.0258	0.0426	0.0930	0.1332	0.2100
0.05 sec	0.6000	0.0414	0.0726	0.1764	0.2676	0.4494
0.10 sec	0.6000	0.0498	0.0840	0.1842	0.2628	0.4098
0.15 sec	0.6000	0.0534	0.0876	0.1818	0.2520	0.3810
0.20 sec	0.6000	0.0552	0.0882	0.1752	0.2376	0.3528
0.25 sec	0.6188	0.0557	0.0873	0.1665	0.2221	0.3267
0.30 sec	0.6375	0.0555	0.0854	0.1594	0.2110	0.3073
0.40 sec	0.6750	0.0520	0.0790	0.1438	0.1883	0.2741
0.50 sec	0.7125	0.0470	0.0720	0.1275	0.1674	0.2437
0.75 sec	0.8063	0.0419	0.0629	0.1097	0.1427	0.2072
1.00 sec	0.9000	0.0405	0.0603	0.1062	0.1377	0.1980
1.50 sec	0.9000	0.0270	0.0414	0.0720	0.0936	0.1359
2.00 sec	0.9000	0.0207	0.0315	0.0549	0.0711	0.1026

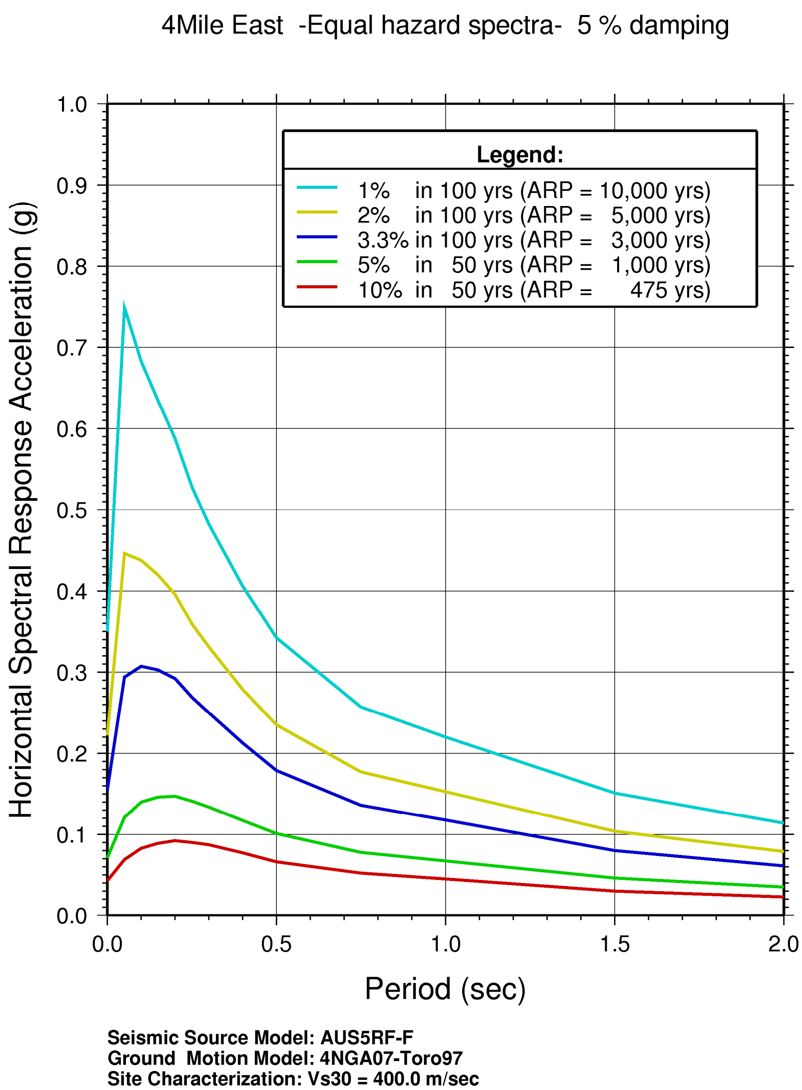

Figure 7. Probabilistic ground motion response spectra at the ground surface at Four Mile East for return periods of 475, 1,000, 3,000, 5,000 and 10,000 years.

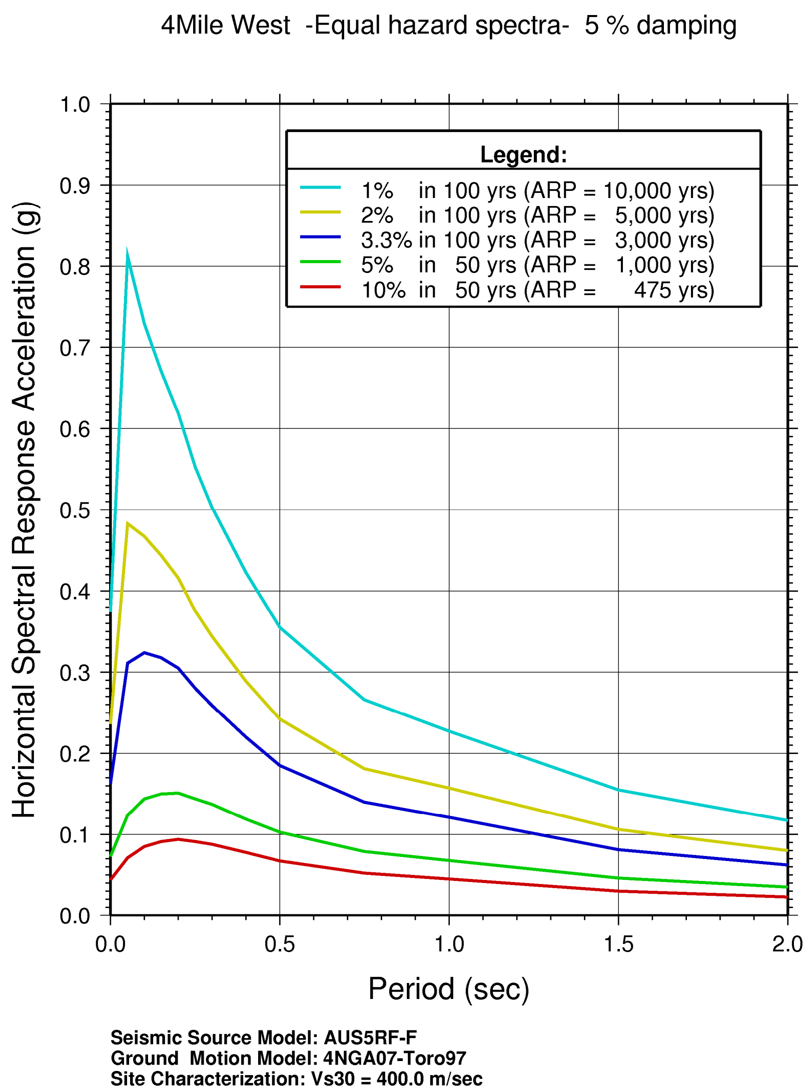

Figure 8. Probabilistic ground motion response spectra at the ground surface at Four Mile West for return periods of 475, 1,000, 3,000, 5,000 and 10,000 years.

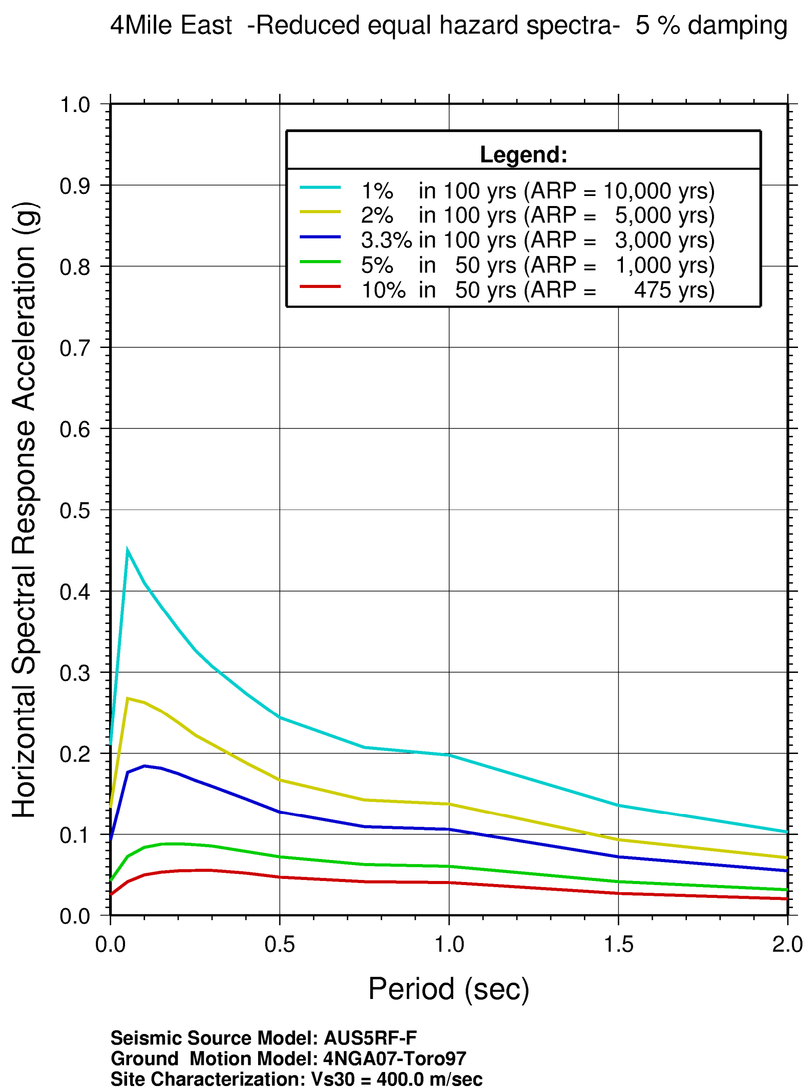

Figure 9. Probabilistic ground motion response spectra at a depth of 180 metres below the surface at Four Mile East for return periods of 475, 1,000, 3,000, 5,000 and 10,000 years.

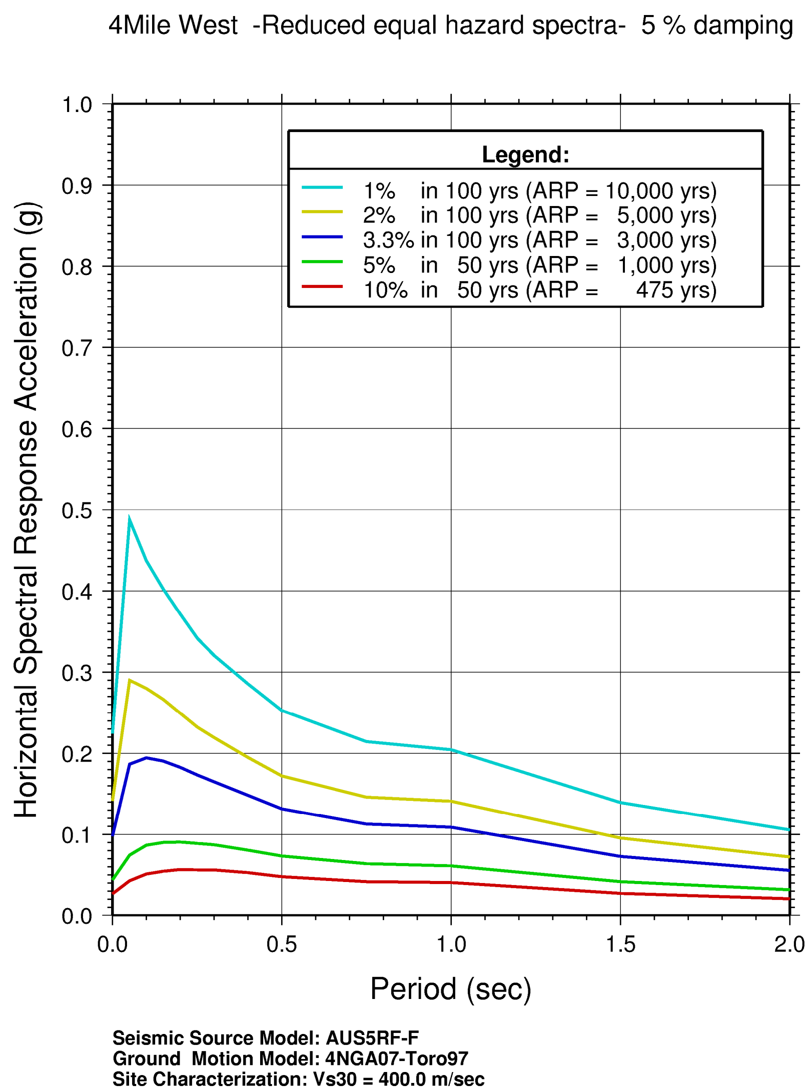

Figure 10. Probabilistic ground motion response spectra at a depth of 180 metres below the surface at Four Mile West for return periods of 475, 1,000, 3,000, 5,000 and 10,000 years.

7.3 Deaggregation of the Probabilistic Seismic Hazard

The hazard curves for peak acceleration, deaggregated by source, are shown in Figures 11 and 12 for the Four Mile East and Four Mile West sites respectively. The slopes of the hazard curves for the three fault sources are relatively shallow, while the slopes of the hazard curves for the distributed source zones are steeper.

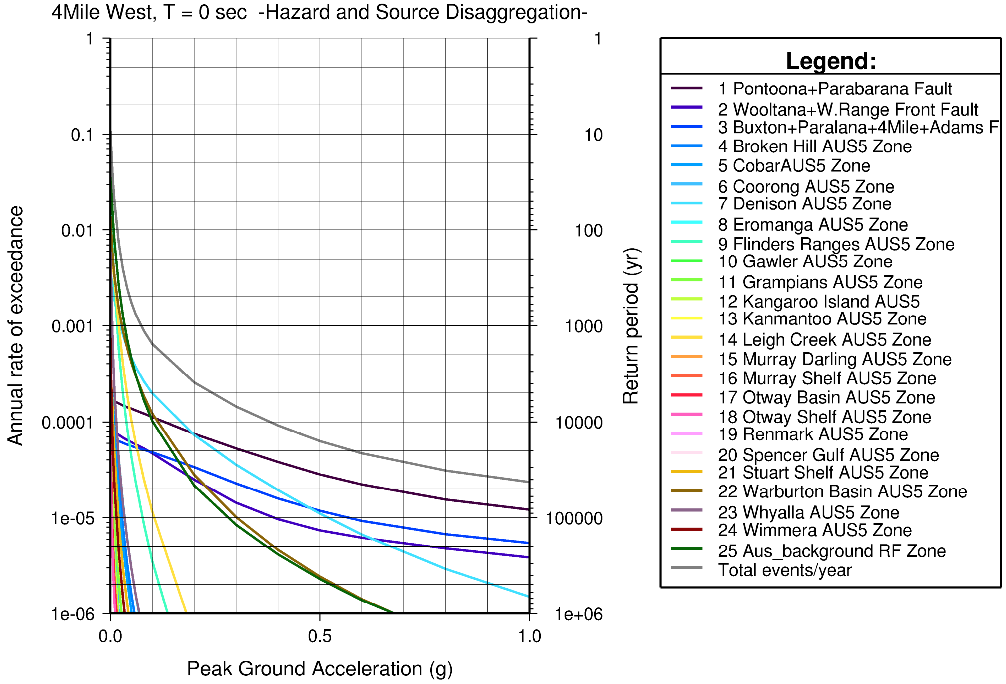

Figure 11. Seismic hazard curves for peak acceleration at Four Mile West.

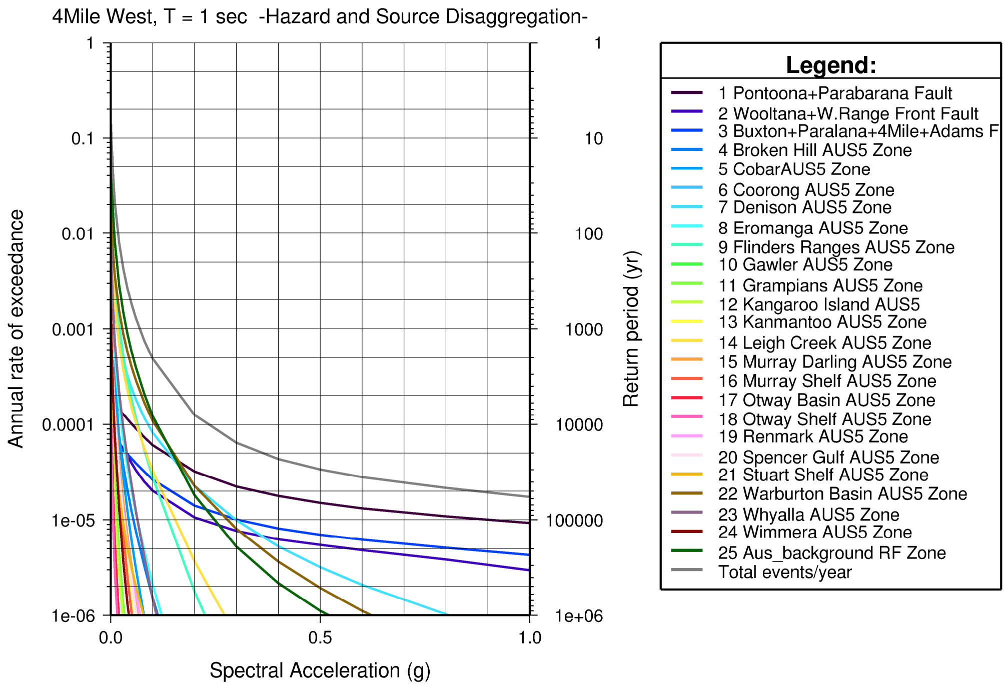

Figure 12. Seismic hazard curves for peak acceleration at Four Mile West.

The distributed sources were represented by two separate models: the updated AUS5 model and the RF model, each with a 50% weight. The hazard curve shows these weighted contributions. The RF model is represented by a single source zone, the Australia background zone. The AUS5 model is represented by numerous source zones.

The hazard curve for the Denison source zone alone in the AUS5 model is higher than the hazard curve for the entire RF source zone for return periods longer than about 3,000 years. For a return period of 500 years, the Denison and Warburton source zones each contribute a hazard level that is comparable to that of the entire RF source zone.

This indicates that the AUS5 source model predicts a higher rate of earthquake activity than the RF source model. The total hazard curve in Figures 11 and 12 represents the sum of the two source model contributions, each weighted at 50%.

At a return period of 500 years, the peak acceleration hazard is dominated by the spatially distributed source zones. The largest contribution to the hazard comes from the Denison zone in which the Four Mile site is located. The neighbouring Warburton zone, at a closest distance of 13 km, also makes a significant contribution to the hazard at 500 year ARP. At this return period, the active faults make a relatively small contribution to the hazard.

At a return period of 10,000 years, the Denison source zone still makes the largest contribution to the hazard, but the Pontoona – Parabarana fault also makes a significant contribution. The other sources making significant contributions to the hazard at this return period are the other two faults, the Warburton zone, and the RF background zone. At return periods longer than 20,000 years, the Pontoona – Parabarana fault dominates the hazard at the site.

The deaggregation of the hazard by earthquake magnitude and distance for peak acceleration and response spectral acceleration at 1 second period is shown for return periods of 475, 1,000 and 10,000 years in Figures 13 through 18 for the Four Mile West site. The deaggregation shows the magnitudes and distances contributing to the probabilistic hazard. The contributions for peak acceleration (zero period response acceleration, Figures 13, 15 and 17) are quite different from those for response spectral acceleration at 1 second period (Figures 14, 16 and 18).

For peak acceleration, most of the hazard comes from earthquakes of magnitudes less than 6 occurring within the distributed earthquake source zones at distances closer than 50 km for a return period of 475 years. This trend is accentuated at a return period of 1,000 years. At a return period of 10,000 years, the predominant earthquake source distances are reduced to 25 km, and there are contributions of magnitude 7 earthquakes on the fault sources.

For 1 second spectral acceleration, most of the hazard comes from larger, more distant earthquakes in very active source zones such as the Leigh Creek zone for return periods of 475 and 1,000 years. This is because large earthquakes generate much larger long period ground motions than small earthquakes, and long period ground motions attenuate more gradually than short period ground motions. At a return period of 10,000 years, the predominant earthquake source distances are reduced to 25 km, and there are large contributions of magnitude 7 earthquakes on the fault sources.

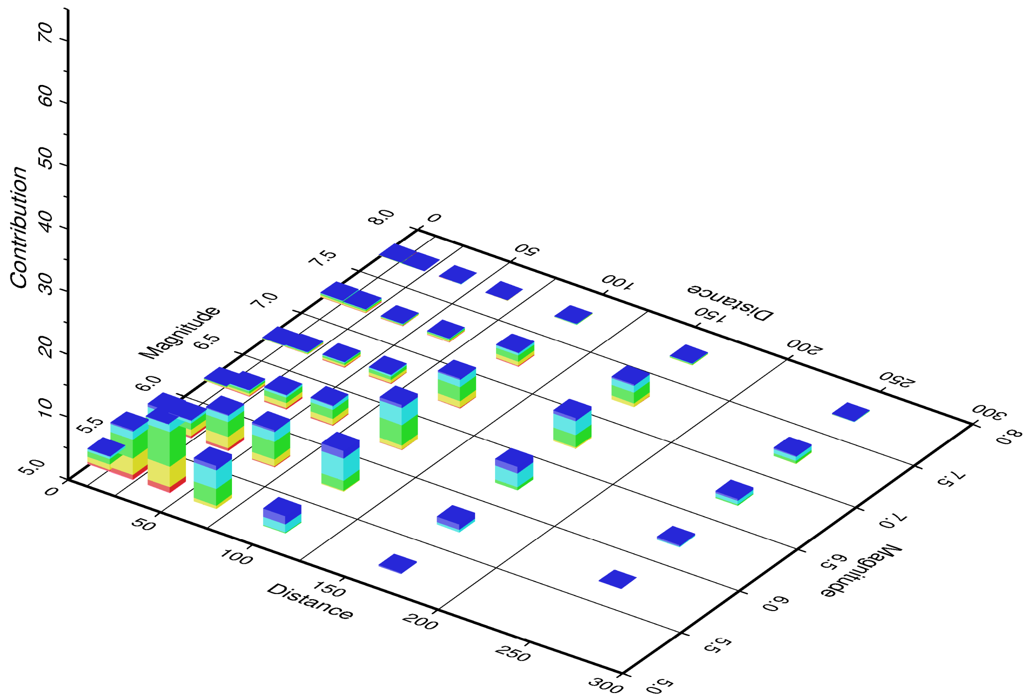

Figure 13. Deaggregation of peak acceleration for 475 year return period.

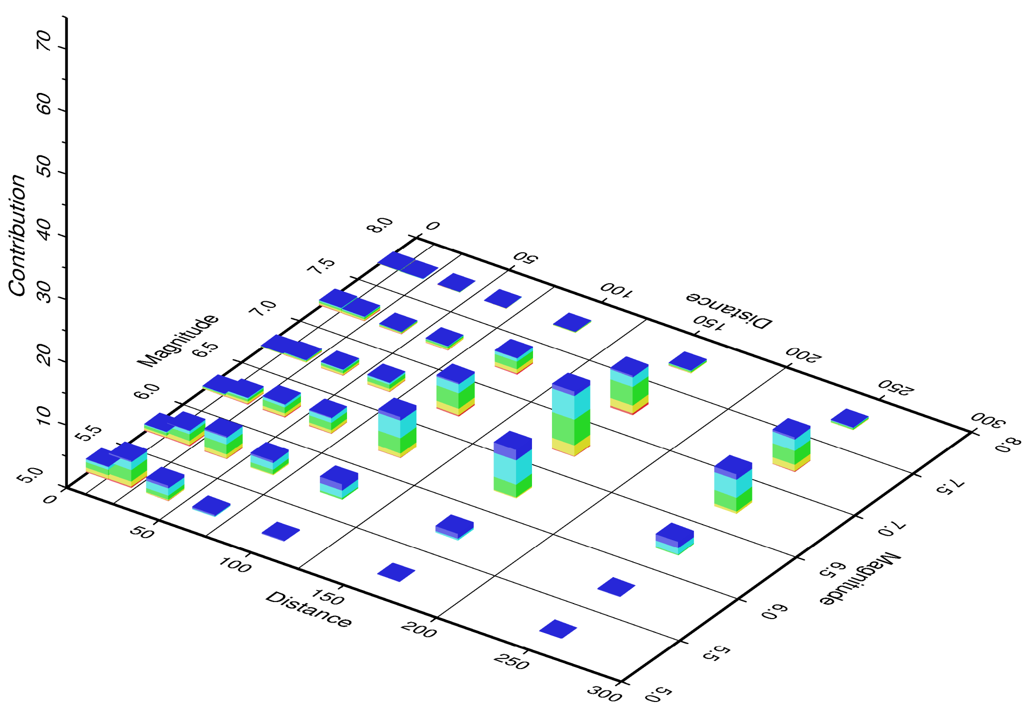

Figure 14. Deaggregation of 1 second period response spectral acceleration for 475 year return period.

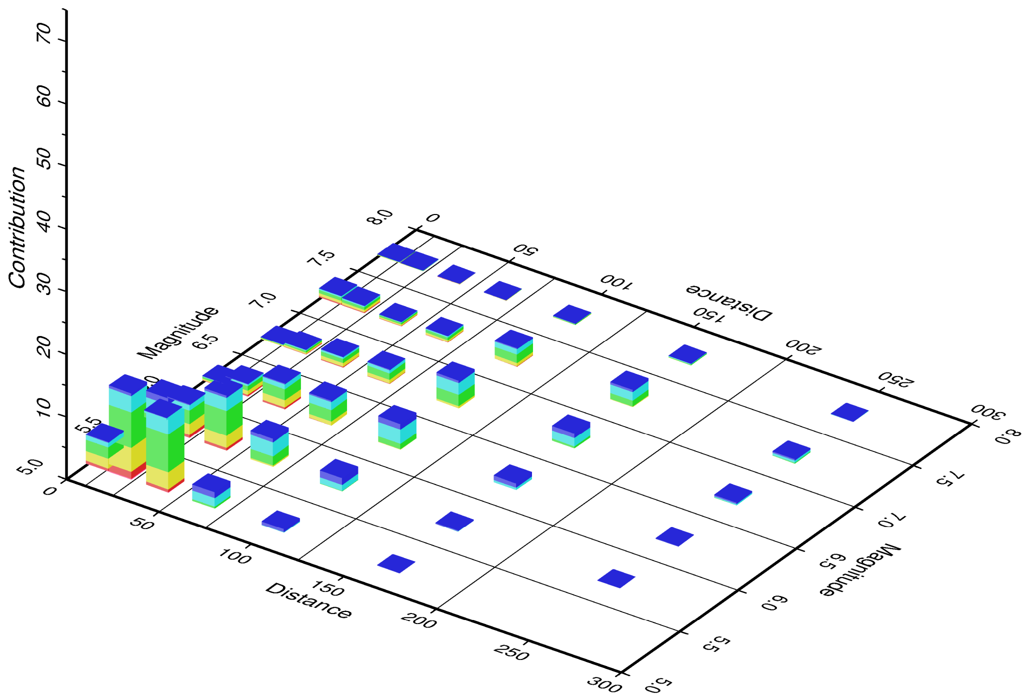

Figure 15. Deaggregation of peak acceleration for 1,000 year return period.

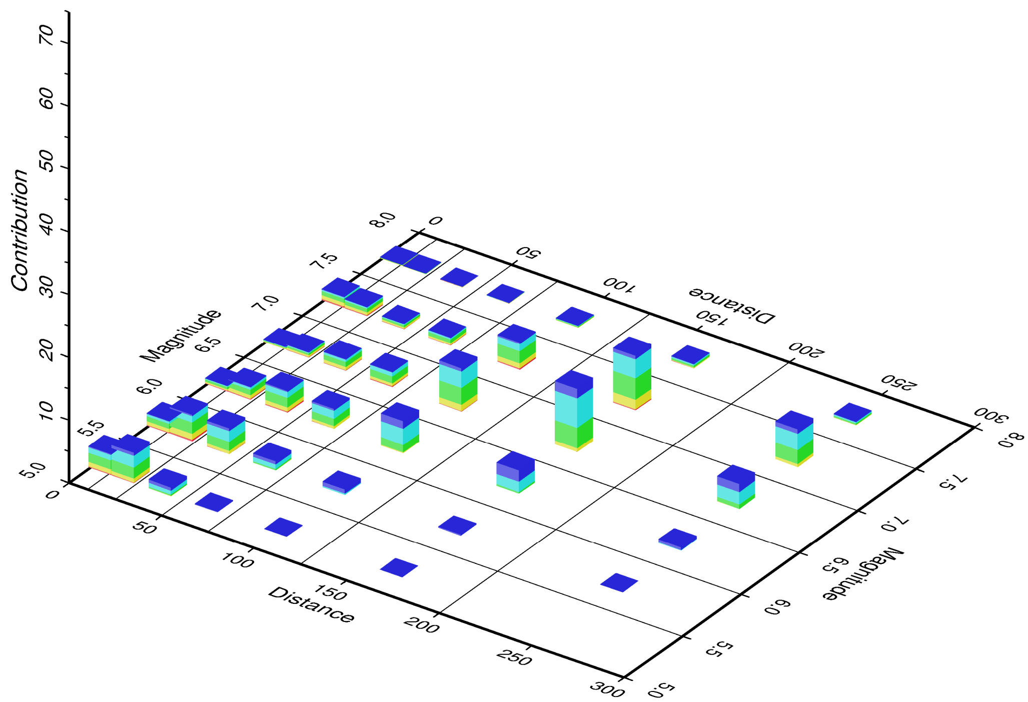

Figure 16. Deaggregation of 1 second period response spectral acceleration for 1,000 year return period.

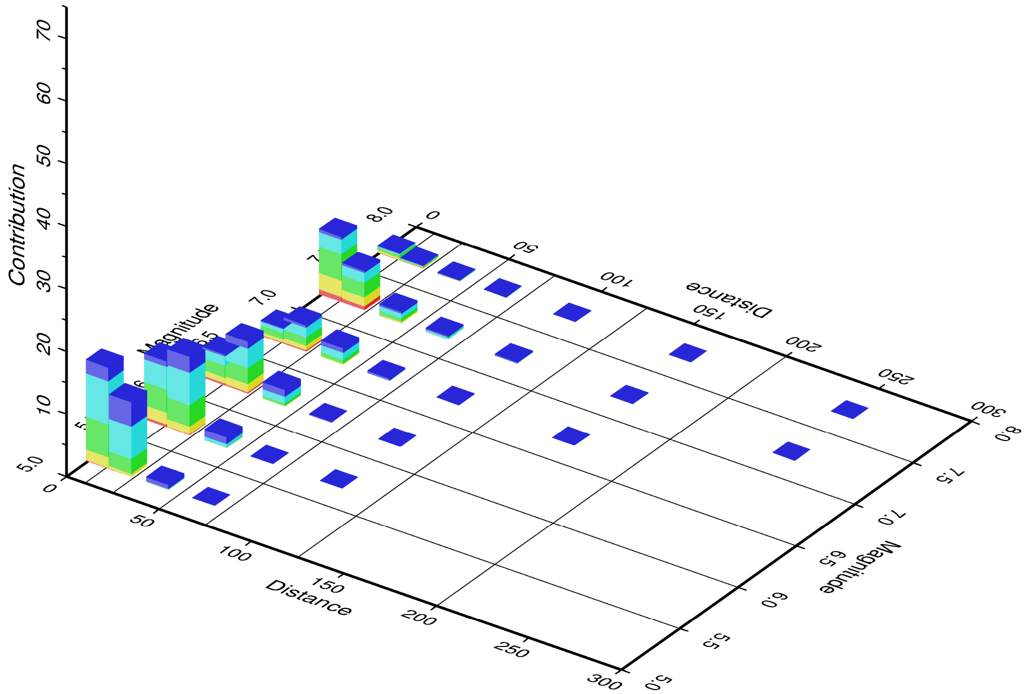

Figure 17. Deaggregation of peak acceleration for 10,000 year return period.

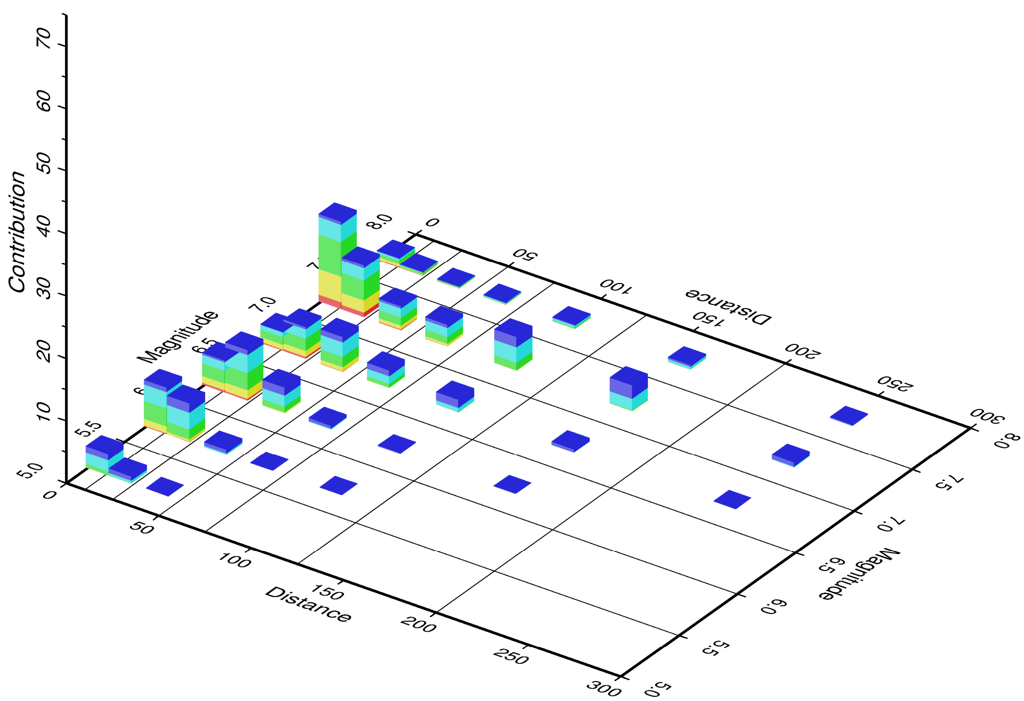

Figure 18. Deaggregation of 1 second period response spectral acceleration for 10,000 year return period.

8. ACKNOWLEDGEMENTS

The summary of active faulting in the site region by Mike Sandiford is gratefully acknowledged. The assistance of Dr Gary Gibson of ES&S in providing the earthquake catalogues and the updated AUS5 earthquake source model, and reviewing the active fault summary of Mike Sandiford, is gratefully acknowledged.

9. REFERENCES

Allen, T.I. and Atkinson, G.M. (2007). Comparison of earthquake source spectra and attenuation in eastern North America and southeastern Australia. *Bull. Seism. Soc. Am* 97, 1350-1354.

Allen, T.I., Cummins, P.R., Dhu, T. and Schneider, J.F. (2007) Attenuation of ground motion spectral amplitudes in southeastern Australia. *Bull. Seism. Soc. Am* 97, 1279-1292.

Allen, T.I., Dhu, T., Cummins, P.R. and Schneider, J.F. Empirical Attenuation of Ground-Motion Spectral Amplitudes in Southwestern Western Australia. *Bull. Seism. Soc. Am*. 96, No. 2, pp. 572–585, April 2006, doi: 10.1785/0120040238.

Allen, T., P.R. Cummins, T. Dhu, and W. Peck (2005). Ground motion attenuation modeling in Australia: implications for earthquake hazards and risk. *Proceedings of the 2005 AEES Conference,* Albury, 41-1 – 41-7.

Abrahamson N.A. and Silva W.J. (1997), Empirical response spectral attenuation relations for shallow crustal earthquakes, *Seis Research Ltrs*; 68(1): 94-127.

Abrahamson N.A. and Silva W.J. (2008), Summary of the Abrahamson & Silva ground motion relations, *Earthquake Spectra* 24, 67-98.

Bakun, W.H., and A. McGarr (2002). Differences in attenuation among the stable continental regions, *Geophys. Res. Lett.* 29, DOI 10.1029/2002GL015457.

Boore, D.M. and G.M. Atkinson (2008). Ground motion prediction equations for the average horizontal component of PGA, PGV and 5% damped PSA at spectral periods between 0.01s and 10.0s. *Earthquake Spectra* 24, 99-138.

Brown, A. and G. Gibson (2000). Reassessment of earthquake hazard in Australia, Proc 12th World Conf on Earthquake Engineering, Auckland, paper 751, 8 pages.

Brown, A. and G. Gibson (2004). A multi-tiered earthquake hazard model for Australia. *Tectonophysics 390*, 25-43.

Campbell, K.W. and Y. Bozorgnia (2008). NGA ground motion model for the geometric mean horizontal component of PGA, PGV, PGD and 5% damped linear elastic response spectra for periods ranging from 0.01 to 10 seconds. *Earthquake Spectra* 24, 139-172.

Campbell, K.W. (2003). Prediction of strong ground motion using the hybrid empirical method and its use in the development of ground-motion (attenuation) relations in eastern North America, *Bull. Seism. Soc. Am.* 93, 1012-1033.

Campbell K.W., and Bozorgnia Y, (2003), Updated near-source ground motion (attenuation) relations for the horizontal and vertical components of peak ground acceleration and acceleration response spectra, *Bull. Seism. Soc. Am.*, 93(1):314-331.

Chiou, B.S.-J. and R.R. Youngs (2008). An NGA model for the average horizontal component of peak ground motion and response spectra. *Earthquake Spectra* 24, 173-216.

Clark, D. (2006). A seismic source zone model based on neotectonics data. *AEES Conference, Earthquake Engineering in Australia,* Canberra, 24-26 November.

Cummins, P., C. Collins, A. Bullock, and D. Love (2008). Monitoring of earthquakes in the Flinders Ranges, South Australia, using a temporary seismometer deployment. http://www.ga.gov.au/image_cache/GA10013.pdf

Frankel, A., C. Mueller, T. Barnhard, D. Perkins, E. Leyendecker, N. Dickman, S. Hanson and M. Hopper (1996). National Seismic Hazard Maps, June 1996. *U.S. Geological Survey Open File Report* 96-532.

Gaull, B.A., Michael-Leiba M. and Rynn J.M.W. 1990. Probabilistic earthquake risk maps of Australia. *Australian Journal of Earth Sciences* **37**, 169-187.

Gibson, G. (2008). Review of Regional Seismicity and Earthquake Source Models, Northern Flinders Ranges. Report to URS, 7 October 2008.

Hall, L., F. Dimer and P.Somerville (2007). A Spatially Distributed Earthquake Source Model for Australia. Proceedings of the 2007 Annual Meeting of the Australian Earthquake Engineering Society.

Heathgate (2008). Beverley Four Mile Public Environment Report – Hydrogeology Chapter 1st Draft, 14 November 2008.

Hu, J.J. and L.L. Xie (2004). Variation of ground motion with depth. Acta Seismologica Sinica 18, 72-81.

Leonard, M. (2008). One hundred years of earthquake recording in Australia. *Bull. Seism. Soc. Am.*, in press.

Leonard, M. and D. Clark (2006). Reconciling neotectonic and seismic recurrence rates in SW WA. *Earthquake Engineering in Australia*, Canberra 24-26 November.

McPherson, A. and T. Allen (2006). An improved understanding of ground shaking in Australia. Proceedings of the 2006 AEES Conference, Canberra, 239-244.

Ninis, D. and G. Gibson (2006). Developing a seismotectonic model using neotectonic setting and historical seismicity – application to central NSW. *AEES Conference, Earthquake Engineering in Australia,* Canberra, 24-26 November.

Quigley, M.C., M.L. Cupper, and M. Sandiford (2006). Quaternary faults of south-central Australia: palaeoseismicity, slip rates and origin. Australian Journal of Earth Sciences 53, 285-301.

Sadigh, K., Chang, C.-Y., Egan, J.A., Makdisi, F. and Young, R.R. 1997. Attenuation relationships for shallow crustal earthquakes based on California strong motion data. *Seismological Research Letters* **68**, 180-189.

Sandiford, M. (2008). Review of Active Faults in the Four Mile Region. Report to URS.

Somerville, P.G. (2008). Source Models of Australian Earthquakes. Draft Report to Geoscience Australia, October 7, 2008.

Somerville, P., N. Collins, N. Abrahamson, R. Graves, and C. Saikia (2001), Ground motion attenuation relations for the central and eastern United States, *Final Report to the USGS, June 30, 2001,* URS Group, Inc., Pasadena, CA, 36 pp.

Toro, G.R., Abrahamson, N.A. and Schneider, J.F. 1997. Model of strong ground motions from earthquakes in central and eastern North America: best estimates and uncertainties. *Seismological Research Letters* 68(1), 41-57.

URS Corporation (2007). Four Mile Project – Concept Evaluation Study. Confidential report to Quasar Resources, 24 October 2007.

Weichert, D. (1980). Estimation of the earthquake recurrence parameters for unequal observation periods for different magnitudes. *Bull. Seism. Soc. Am*. 70, 1337-1346.

ATTACHMENT 1. Review of Active Faults in the Four Mile Region

by Mike Sandiford

Four Mile Creek Report for URS

Compiled by Mike Sandiford
School of Earth Sciences
University of Melbourne

Review of Active Faults in the Four Mile Site Region

Directive: Review the published literature for information on active faults in the vicinity of the site, including the Paralana fault described by Sandiford (2003) and the Mt Jacob (or Wooltana) and Poontana faults. Information of interest includes orientation, style of faulting, deformation (e.g. uplift) rates, and fault slip rates, together with displacements, estimated magnitudes and recurrence intervals of paleoseismic events. This information will be used by URS to develop earthquake source models for the ground motion analysis, and to assess the potential for surface faulting at the site.

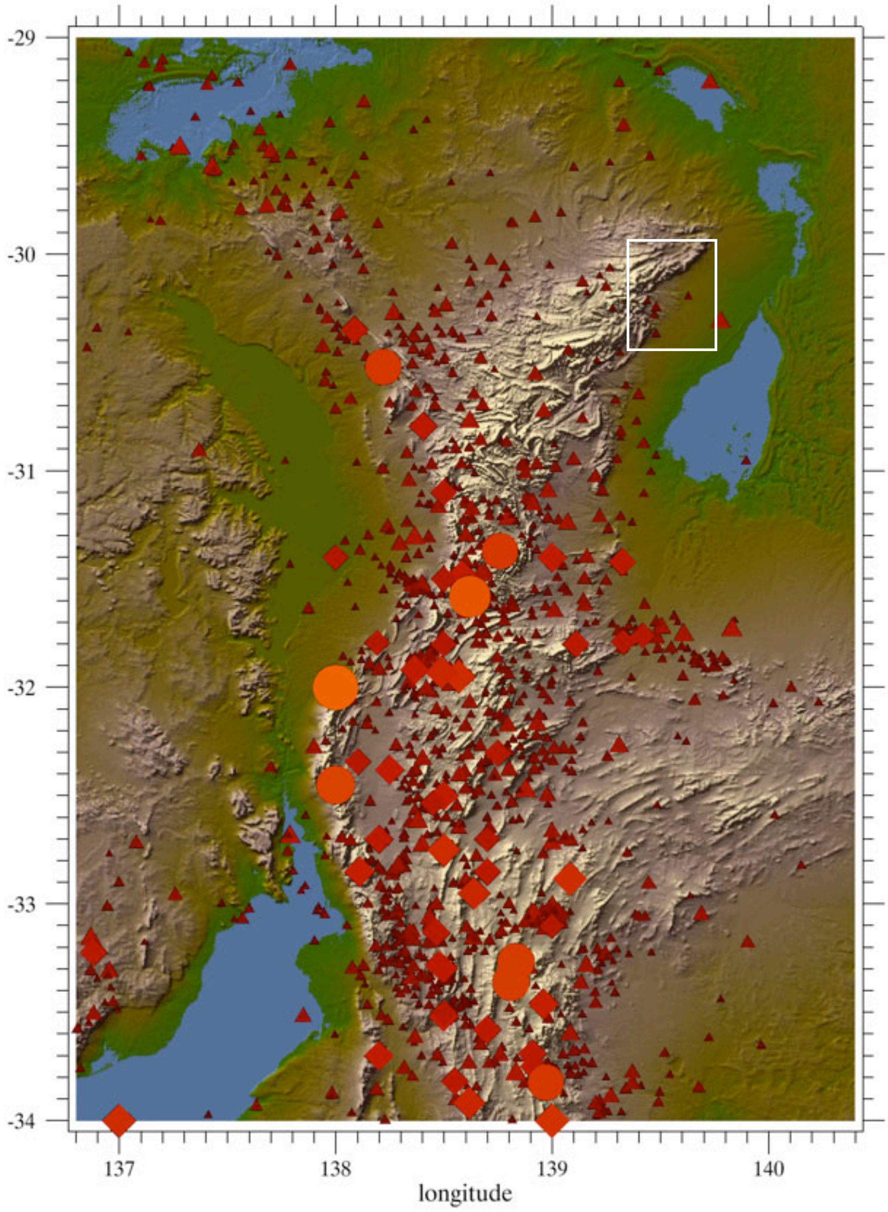

Earthquake distribution in the Northern Flinders Ranges. Triangle ML <4, diamons, ML 4-5, Circles, ML > 5. Four mile creek region indicated by square.

1. Introductory comments

Four Mile Creek forms an ephemeral drainage system incised into the Paralana escarpment and the adjacent Paralana High Plains, on the eastern side of the Mount Painter Inlier in the Northern Flinders Ranges. Like many parts of the Flinders Ranges, the abrupt nature of the Paralana escarpment suggests it coincides, at elast in part, with an active fault system, consistent with the relatively frequent occurrence of earthquakes in many other parts of the ranges.

In terms of historical seismicity the number of earthquakes in the Mount Painter region is not significantly above background rates and the relationship between abrupt relief and active tectonics is somewhat more questionable than in regions such as the Wilkatana area (eg. Quigley et al., 2006). However extensive field studies by myself and students in my group have revealed a number of outcrops that conclusively demonstrate young fault motion. Precise dating of fault movements has proved difficult because of the intense background radiation due to elevated natural levels of Uranium, and thus the history of fault motion at individual localities is not well constrained. However, quantitative measures of erosion rates do place general constraints on timing and rates of fault slip. In sum, the evidence is for active faulting along the Paralana escarpment as well as several faults that uplift the outwash fans of the Paralana High Plains.

This report summarises the body of field work and analytical data collected by Prof Mike Sandiford and his students over a period of more than 15 years between 1992-2007. Much of the work is synthesised from student theses, under Sandiford's supervision, and associated publications (see attached reference list).

Evidence for active or recently active (last few million years) faulting in the vicinity Four Mile Creek, is provided by several observations, namely:

- direct exposures of faults along the Paralana escarpment
- offsets of outwash gravels on the Paralana High Plains
- evidence for relatively rapid incision in the Yudnamatana Gorge from measured concentrations of cosmogenic nuclides.

Each of these items is addressed in this report.

2. **Fault exposures on the Paralana escarpment**

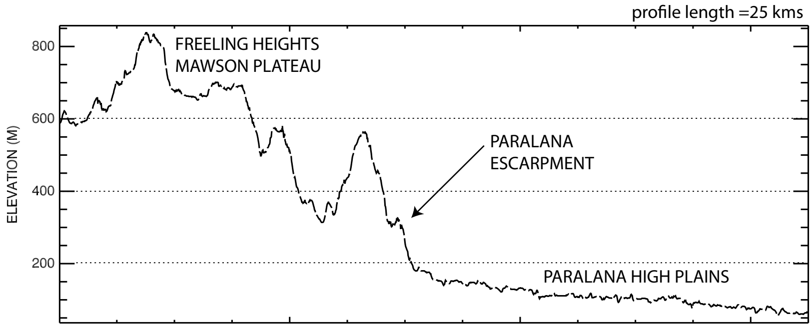

Top: view north along Paralana escarpment from Sillers Lookout. **Bottom**, topographic profile across Paralana escarpment in the vicinity of Four mile Creek.

Main references
Celerier, 2002
Celerier et al., 2005

The Paralana escarpment defines the eastern range front, marking the boundary between crystalline rocks of the Mount Painter Inlier and late Neogene (< ~ 5 Ma) outwash gravels of the Paralana High Plain. Typically, relief across the Paralana escarpment is about 400 m. Our mapping has revealed several localities on and near the escarpment that show evidence for reverse fault offsets between 'basement' rocks to the west and Tertiary and/or Quaternary sediments to the east including hill screes. The most spectacualr by far is the 'Teasdale' Locality - so named after Jon Teasdale who discovered this outcrop as part of his honours mapping in 1993. This locality is one of the most impressive demonstrations of active thrust faulting in the Flinders Ranges. It is approximately 1 kms north of Four Mile Creek, on the northern side of a small creek as it exits through the Paralana escarpment. It clearly evidences thrust faulting of basement over younger sediment along a fault plane sub-parallel to the range front. The Teasdale locality displays several faults distributed in a ~5 m wide zone. The footwall of the structure hosts very angular, poorly sorted conglomerates presumed to be of the Willawortina Formation. In the footwall, these gravels are overlain by a 6 m wide, by 2.5 m high wedge of faulted scree. The footwall screes can be traced upward with no obvious dicsontunity into a .5-1.0 m thick scree mantle that cloaks the entire outcrop including the fault. The strike of the basal thrust is 012°, with a dip of 25° to the west. Kinematic indicators along the plane confirm the reverse sense of movement. Fault groove lineations trend down dip implying dip-slip motion. The hangingwall comprises several reverse faults with varying orientations. Total displacement within the fault zone is difficult to quantify with any great accuracy. Given that the thrust places Mesoproterozoic basement and possibly Eyre Formation above Willawortina Formation, a rudimentary approximation of recent displacement can be estimated. Callen & Tedford (1974) show that the Willawortina Formation reaches a thickness of 150 m. To account for the present relationships, in the order of 150 m of vertical displacement must have occurred since deposition of the Willawortina Formation during the Pliocene. Youthful, neotectonic movement along the structure is implied by the ~2.5m thick wedge of hill scree in the footwall, topped by aan ~ 8 m long fault trace. Given that the red hill scree overlies Pliocene Willawortina Formation, the most recent episode of faulting must have occurred after deposition of the red hill scree, at some stage during the Quaternary. Since the fault is draped is by the youngest screes, its most recent movement clearly predates the most recent epsidoe of scree formation.. Attempts to constrain a maximum age of the fault

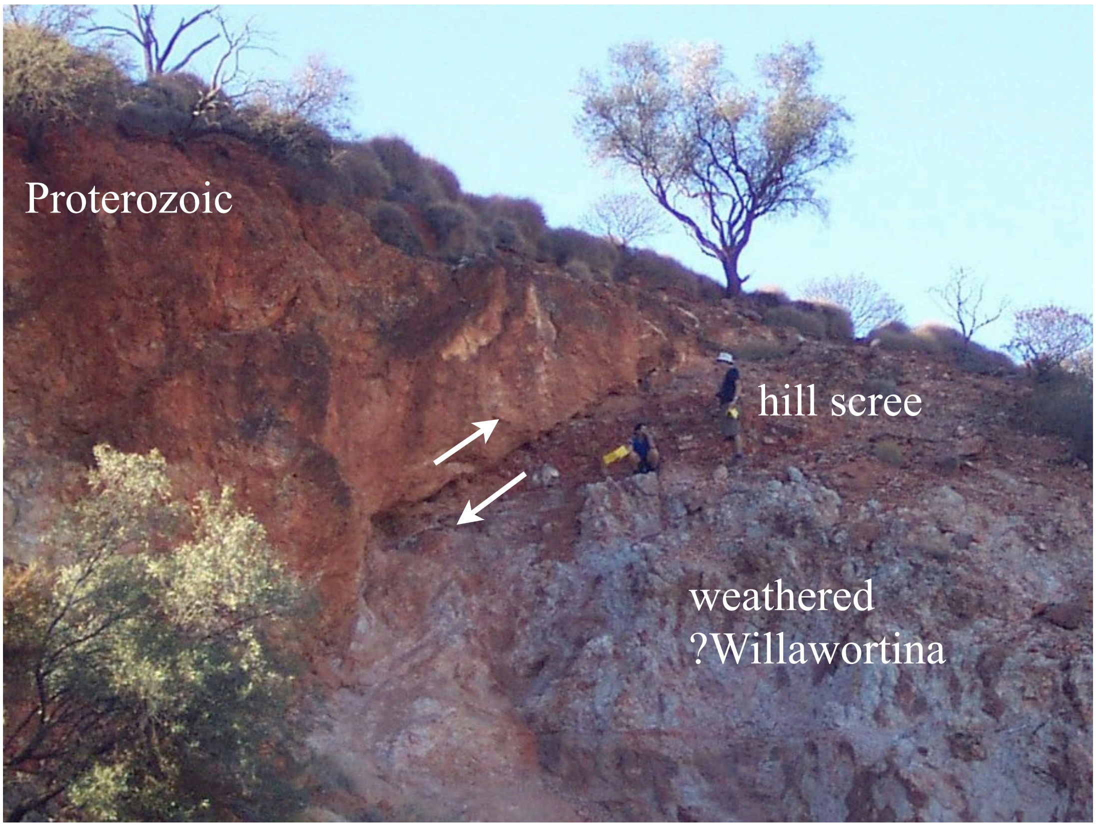

Photo of theTeasdale locality, view to the north.

by dating the wedge of hill scree using optically stimulated luminescence (OSL), have proved inconclusive showing that the wedge of hill scree in the thrust footwall is no younger than 36,000 years old.

Several other localities show young reverse fault motion placing basement rocks above younger sediment on or near the Paralana escarpment. One of the most accessible is at Lady Buxton Mine, along the track leading to the Paralana Hot Springs, where excavations associated with mining have exposed a thrust on the western side of the Paralana Hot Springs track. The footwall of the thrust comprises a well consolidated ferruginous conglomerate characterised by sub-angular to sub-rounded, poorly sorted polymictic clasts 10 cm in diameter. Since the clasts include Mesoproterozoic and Neoproterozoic material, as well as maghemite pebbles, in a

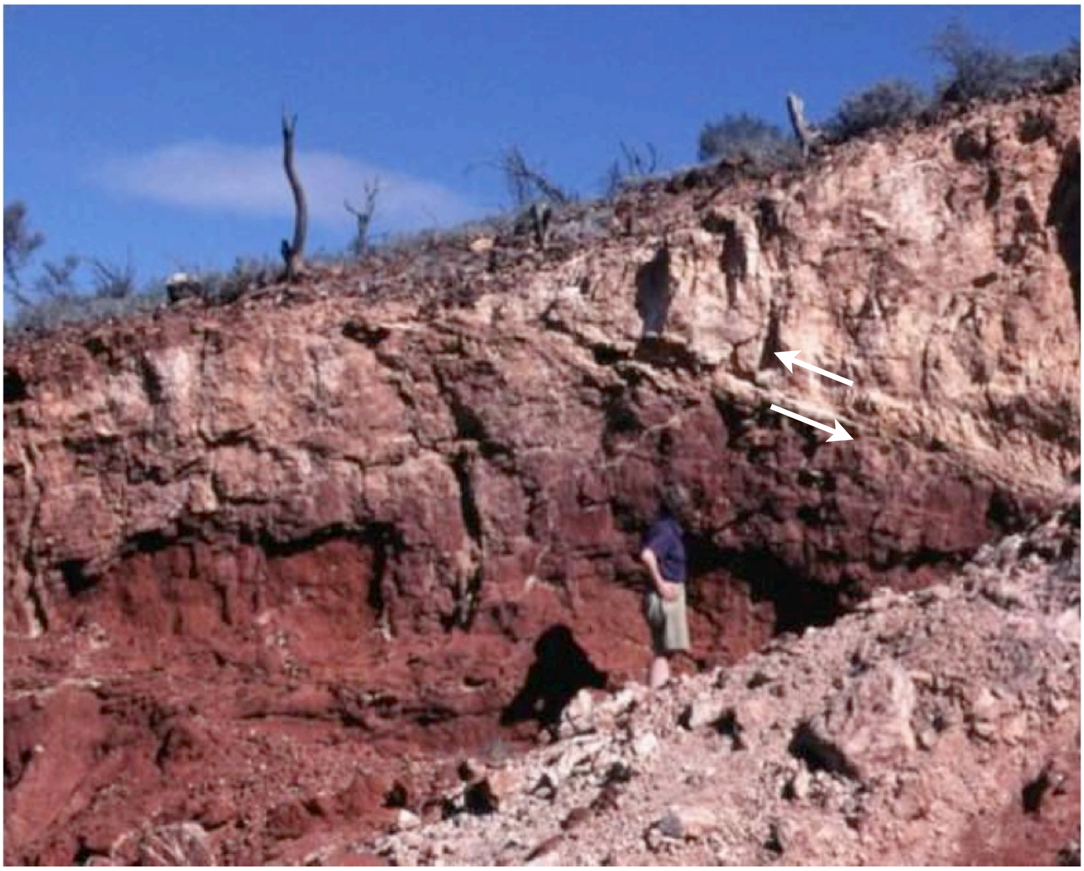

Photo of the Lady Buxton locality, view to the south.

matrix of sandy to gritty quartz cemented by ferruginous matter, it is considered to be Cainozoic in age. The hangingwall comprises weathered Neoproterozoic marbles of the Wywyana Formation. The thrust is oriented 074° and dips at 19° toward the north-west (Figure 3.4). Linear grooves on the fault plain trend down dip, suggesting purely dip-slip movement. An estimate of displacement along the structure is problematic as the thickness of the footwall sequence is unknown. The age of the faulting is poorly constrained as the footwall lithology is unique within the field area, only being encountered at this locality.

Celerier (2002) reports three additional localities along the escarpment between Paralana Creek and Mount Parabarana in the north where mapping requires thrusting of basement over out-wash gravels, including the locality illustrated in the South Australian Geological Survey Bulletin 54 (Drexel & Price, 1995; Love et al., 1995).

TOP: DEM of the

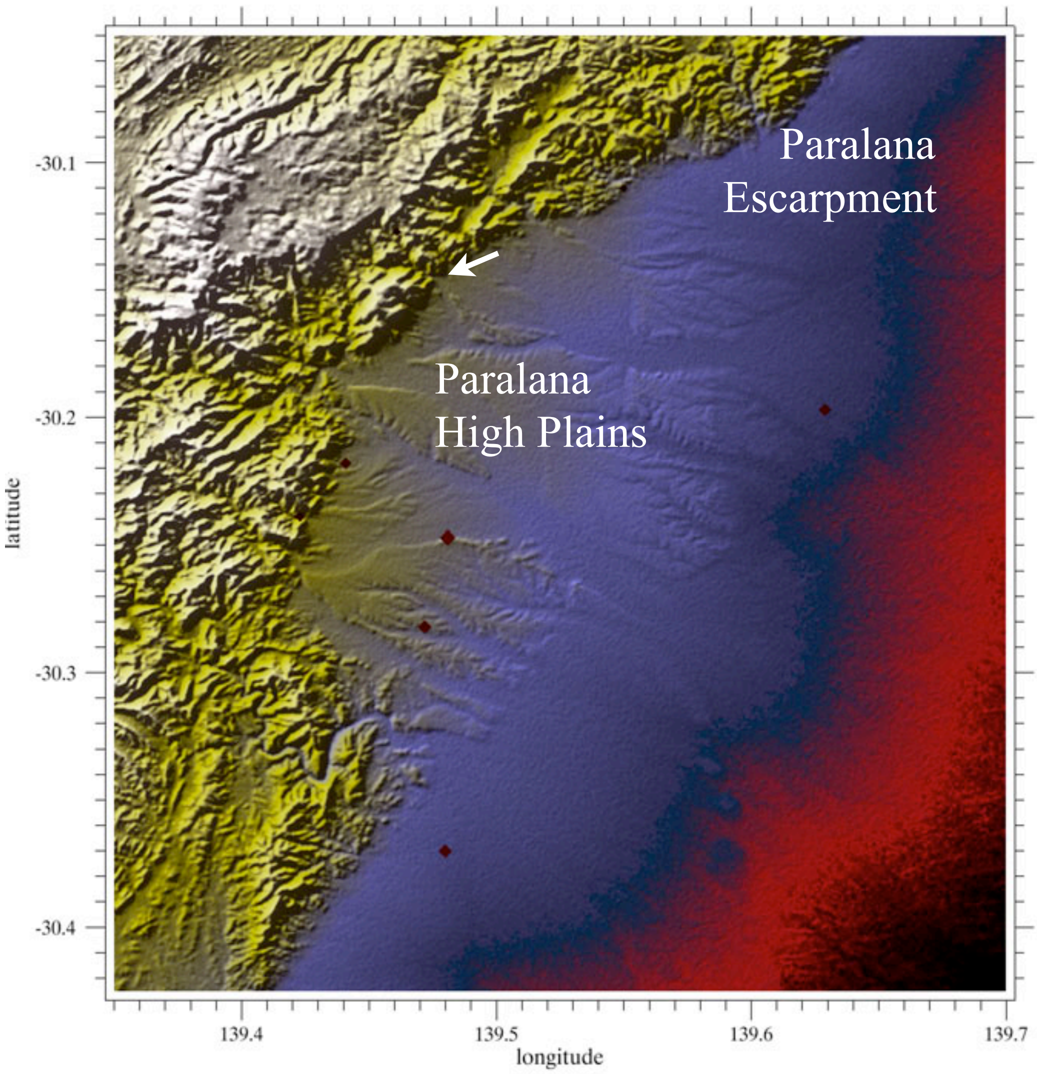

TOP: DEM of the Paralana High Plains. arrow shows loclaity of faulted four mile creek outcrop.

BELOW: Interpolation of fault evolution on Paralana High Plains after Harper, (2002), showing how faults demarcate the bioundary between incised and distributory channel systems.

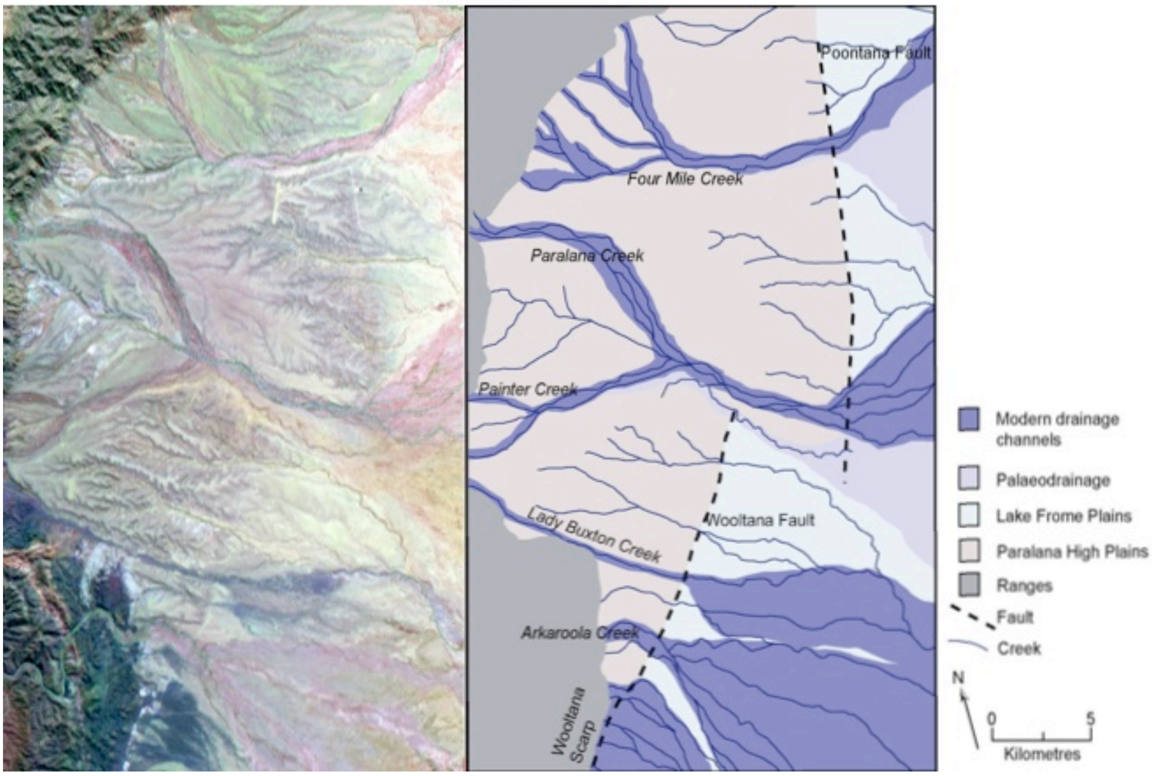

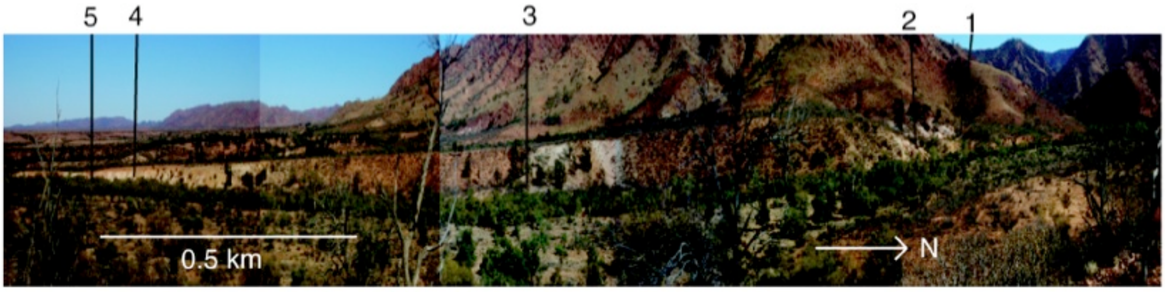

TOP: view to the south of incised alluvial fan sequences in Four mile creek, near the Paralana escarpment.

BOTTOM: small reverse fault cutting older Willawortina gravels in Four Mile Creek.

3. The Paralana High Plains

Main references
Elliot, 2002
Harper, 2002
Petts, 2002

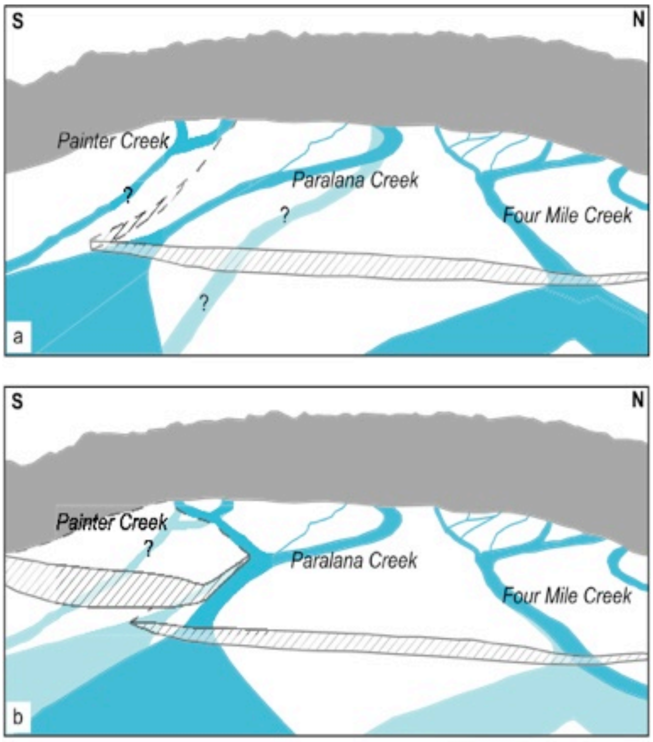

Schematic of the fault related history of the Paralana High Plains from Harper (2002)

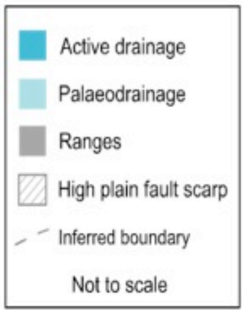

The Paralana High Plains (PHP)are a region of dissected out-wash alluvial fans bounded to the west by the Paralana escarpment and to the east by linear features in the landscape associated with small (~10 m) vertical offsets in theupper surface of the fans. These also mark the transition from incised channel forms to the west to distributory channel forms to the east (eg. in Arkaroola, Paralana and Four Mile Creeks).

Several lines of evidence suggest the dissection of the plains was triggered by active faulting.

The southern linear feature aligns with the continuation of the eastern range front in the vicinity of Wooltana. While there is no documented clear evidence that the Wooltana (or Mount Jacob) scarp is active, or has been recently active, it morphological similarity with the Paralana scarp suggests that it most probably is. This fault segment has been termed as the Wooltana Fault in our studies, including the segment that continues beneath the out-wash gravels. It probably coincides with what others have called the Mt Jacob Fault.

The north-eastern boundary of the Paralana High Plains, also has the form of linear faults scarp and is related to the Poontana Fault. The unconsolidated nature of the uppermost fluvial Willawortina gravels means that fault traces are quickly degraded, and we have not observed any direct surface outcrops of these fault planes.

A second line of evidence is more direct in the form of clear exposure of a reverse fault in an incised section of older, consolidated and more deeply weathered section of the Willawortina gravels in Four Mile Creek, near the range front. This outcrop clearly shows an offset of ~1m of dip-slip reverse motion on 40° west-dipping plane.

Harper (2003) carried out detailed analysis of ASTER satellite data over the Paralana High Plains and there equivalents near Balcanoona further South. She interpreted the history of palaeodrainage, across the Paralana High Plains as showing sequential faulting, involving firstly movement on the Poontana Fault followed by movement on the Wooltana Fault.

Elliot (2003) carried out detail mapping of stratigraphy of Willawortina gravels a exposed in the incised valley systems of the Paralana and Four Mile creeks. Petts (2003) undertook a detailed geomorphic mapping of the Paralana High Plains dosumenting numerous episodes of incision and aggradation.

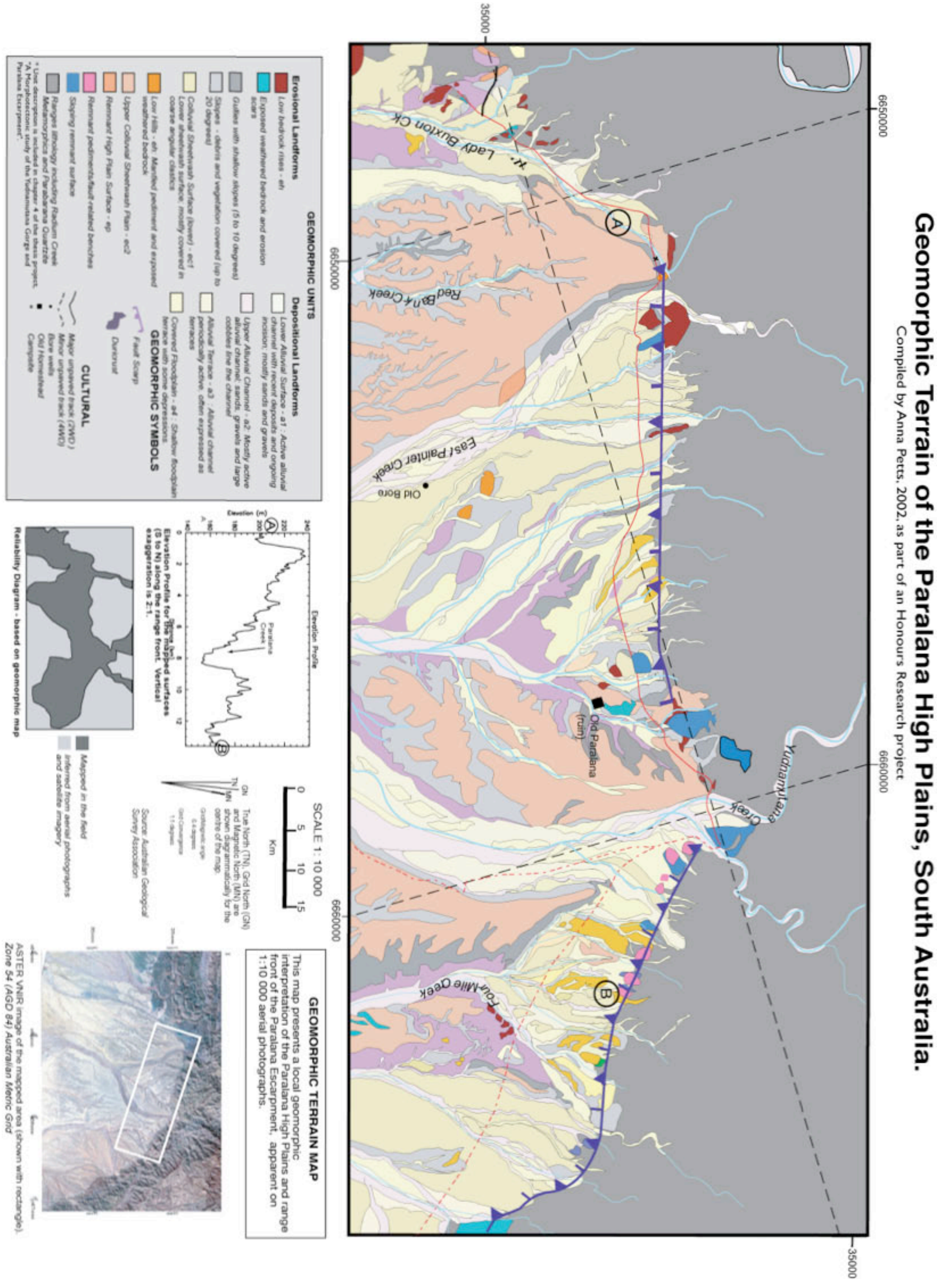

4. **Yundamatana Gorge**

Main reference
Quigley et al (2007a)

Cosmogenic Be concentrations in exposed bedrock surfaces and alluvial sediment can be used to estimate the rate of erosion, and show how for example relief has developed in time in incised valleys such as those that cross the Paralana escarpment. Quigley et al. (2007a) reported measurements of 10Be in alluvial sediment and bedrock surfaces from the Yudnamatana Catchment. These measurements show that bedrock erosion rates increase with decreasing elevation in the Yudnamutana Catchment, from summit surfaces (13.96 ± 1.29 and 14.38 ± 1.40 m /Myr), to hillslopes (17.61 ± 2.21 to 29.24 ± 4.38 m/Myr), to valley bottoms (53.19 ± 7.26 to 227.95 ± 21.39 m/Myr) indicating increases in topographic relief over Late Quaternary timescales. The erosion rate derived from 10Be concentrations in contemporary alluvial sediment (22.79 ± 2.78 m/Myr) indicates that slowly eroding bedrock surfaces are volumetrically minor relative to more rapidly eroding hillslopes when considered on the scale of the Yudnamatana Catchment. Quigley et al. (2007a) used these data to imply Quaternary relief production of 30-160 m/Myr due to range-front reverse
faulting.

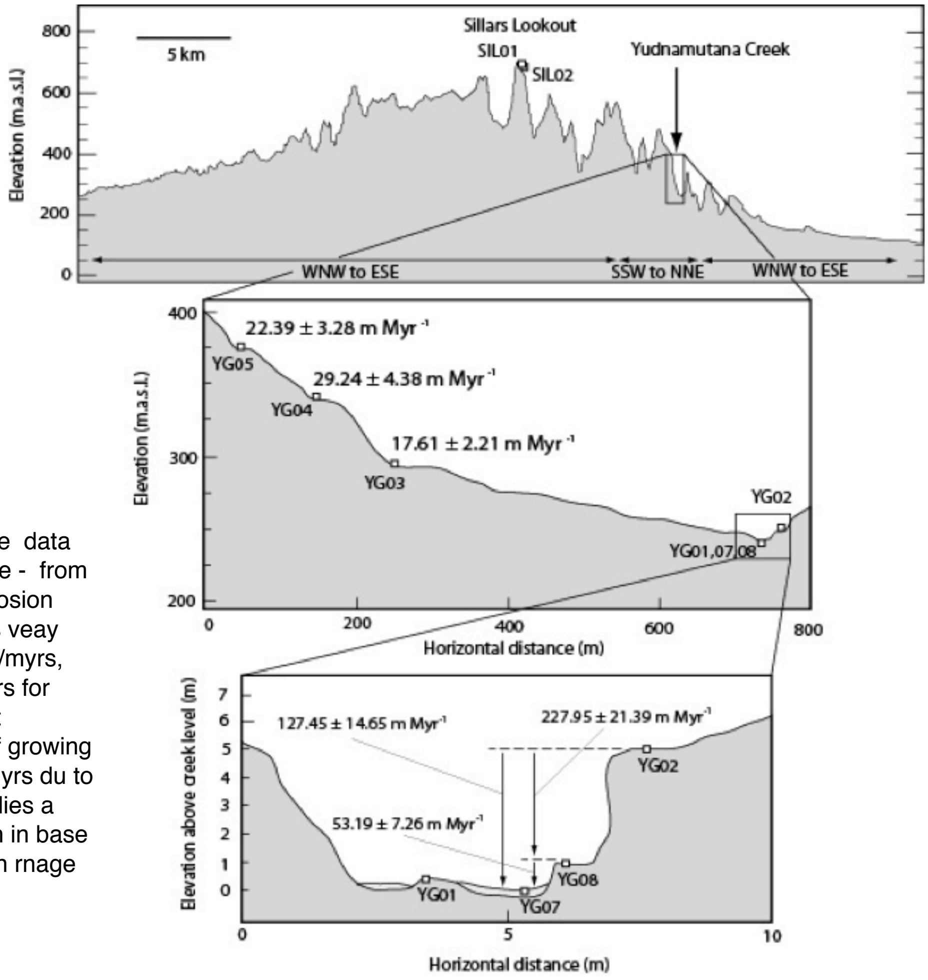

Summary diagram of cosmogenic erosion rate data from Yundnamata Gorge - from Quigley et al (2007). Erosion rates in the valley floors veay form abou 50 to >120m/myrs, compared to ~ 20m/myrs for valley walls and summit surfaces. Implying relief growing at between 30-100 m/myrs du to rviver incision. This implies a corresponding evolution in base level attributed to slip on rnage bounding faults.

5. **Fault geometry**

Despite the observations cited in the previous sections evidencing active or recently active faulting in the Four mile creek region, the geometry of fault ruptures is not well constrained due to lack of continuity of surface expression of fault rupture segments. Below I provide an interpreted fault geometry based on integration of observations cited above, and interpretation of the tectonic geomorphology, bearing in part on experience in other parts of the Flinders Ranges. While the lengths of individual faults strands that might be capable of rupturing in single events are not well constrained, it is clear form observations that the range front comprises a segmented fault system. This is clear from the offset of the Wooltana and Paralana escarpments, from the scalloped shape of the Paralana escarpment, and from the observation at the Teasdale locality that the fault plane is slightly oblique to the range front

The range front along the Paralana escarpment, seems to comprise several fault segments with individual segments typically around 10 kms in length. Geogarphic co-ordinates of faults strands are listed in Appendix 1.

The **Paralana Fault** defines the range front between the Hot Springs and Four Mile Creeks. South of the Paralana Hot Springs, offset in Mesozoic surfaces suggest that it splays into the ranges (Celerier, 2002) along the Yudnamatana Creek. The southern limit s not well defined. North of Four Mile Creek the fault again seems to trend oblique to the range front, probably cutting through it at the Teasdale locality, into the ranges where it may connect with faults in Hidden Valley (or Mount Adams Valley). The total length of the fault is estimated at 16 kms, but maybe as much as 20 kms in length, depending on how far it continues north into Hidden Valley.

The **Buxton Fault** is the main range bounding fault immediately south of Paralana Gorge, extending at least 9 kms along the range front before cutting into the ranges. Its southern termination is not well defined.

Several en-echelon faults strands are probable along the range front to the north of Four Mile Creek including the strands here named as **4mile** and **Adams** (each with lengths of about 6 kms). Further north the range front is defined the Parabarana fault strand with a length in excess of 10 kms. The Parabarana fault strand may well represent a continuation of the Poontana fault.

The rupture lengths of the **Poontana** and **Wooltana** faults are rather better constrained at least where they breach and offset the surface of the Willawortina gravels. The **Poontana** fault is estimated at 15 kms. The **Wooltana** fault extends about 17 kms across the Paralana High plains, but clearly continues further south along the range front near Wooltana and thus may have a rupture lengths in excess of 25 kms.

DEM of the Paralana High Plains. arrow shows loclaity of faulted four mile creek outcrop. approximate position and lengths of faults as shown.
Pa -Paralana, Bu:Buxton, A: Adams, Po:Poontana, W, Wooltana; WRF Wooltana Range Front; 4M, Four Mile; Pb, Parabarana, as mapped by surface geological expressions (Celerier, 2002; Harper, 2002) and geomphic infernces.

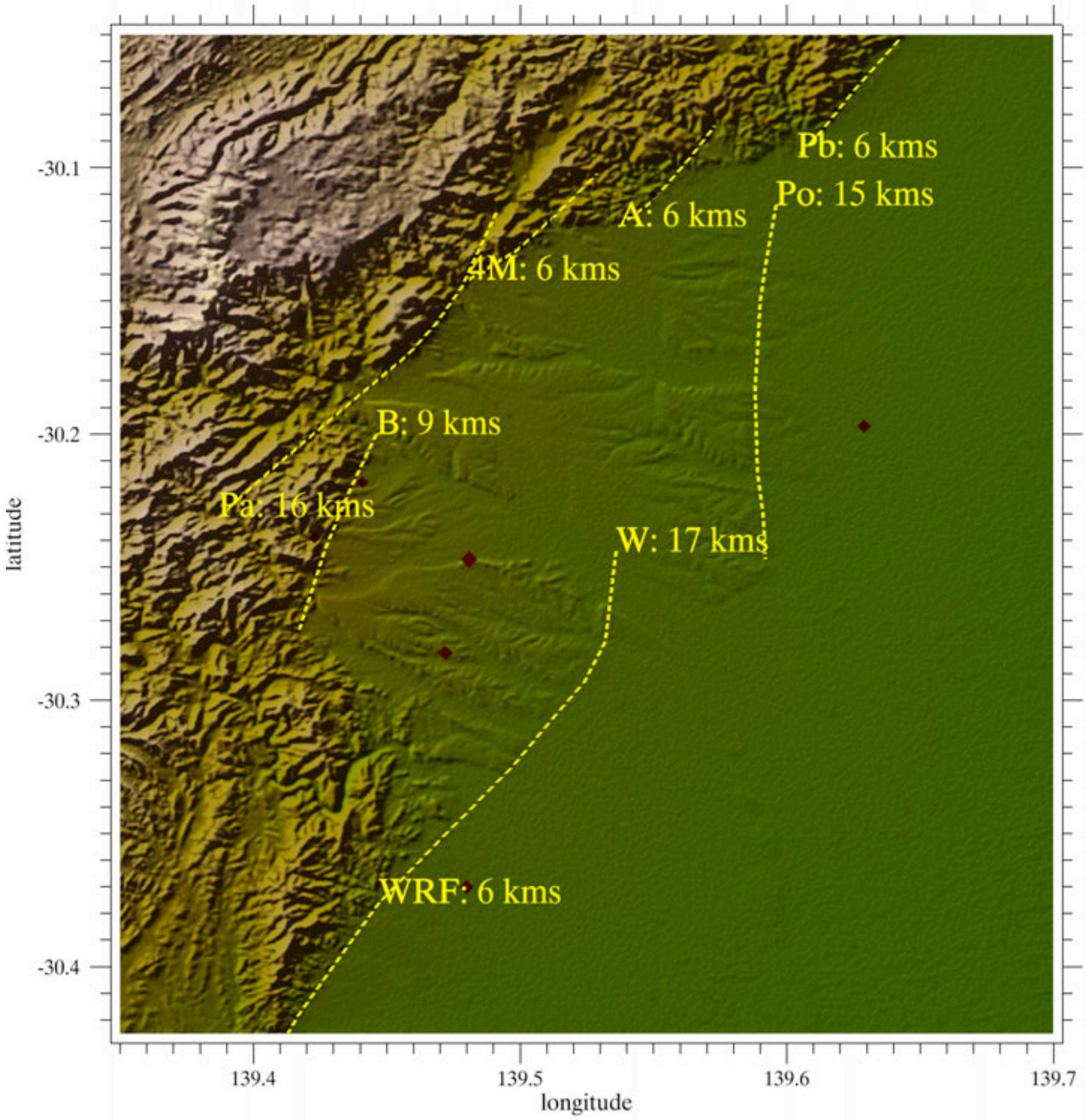

6. **Timing constraints**

OSL dating that have been used successfully elsewhere in the Flinders Ranges to date fault movement (eg., Quigley et al. 2006, 2007b,c). However, the high levels of natural radioactivity mean that OSL is of little use in the Four Mile Creek region (at high levels of radioactivity OSL saturates at doses received on timescales of ~10,000 years, and therefore cannot be used to see back beyond the Holocene). Therefore estimates of fault activity and fault slip rates can only be based on indirect measures such as the erosion rates inferred from cosmogenic studies.

The Poontana and Wooltana faults both displace the youngest of the Willawortina gravels on upper surface of the Paralana High Plains (PHP). No direct age of these gravels is obtained but inferences can be drawn assuming that the incision of the Paralana High Plains has occurred at rates comparable with incision in the Yudnamatana Gorge ie., 30 - 160 m/myrs. With incision levels in the footwall of the range front of about 30 m, the youngest gravels are estimated to be 0.2 - 1 Myr old. Both the Poontana and Wooltana faults clearly displace this PHP surface and thus must have had more recent movement. Total displacement is approximately 10 m, and so slip rates are of the order of 10-50 m/myr.

Total slip on range bounding faults is clearly much greater, and is likely to measure in the hundreds of meters accrued over the last 5 million years or so, comparable with cumulative fault slip determined at Wilkatana and in the Mount Lofty Ranges (Quigley et al, 2006; Sandiford, 2003). It is probably reasonable to assume slip rates balance incision rates in the Yudamatana Gorge, ie. in the range 30-100 m/myrs. At 100 m/myrs, the present relief in Yudnamatana would have grown in the last 5 million years, consistent with the notion first proposed by Callen & Tedford (1976), that the region was characterized by much lower relief in the Miocene during deposition of the Namba Formation (see also, Sandiford 2003).

References.

Callen, R.A. & Tedford, R.H., 1976. New late Cainozoic rock units and depositional environments, Lake Frome Area, South Australia. Transactions of the Royal Society of South Australia 100, 125–167.

Celerier, J., 2002, Neotectonics and intraplate deformation in the northern Flinders Ranges, South Australia, BSc(Hons) thesis, University of Melbourne.

Celerier, J., Sandiford, M., Hansen, D.L., Quigley, M., 2005, Modes of active intraplate deformation, Flinders Ranges, Australia, Tectonics, 24, doi: 10.029/2004&C001679

Drexel J.F & Preiss W.V (eds), The Geology of South Australia, Volume 2, The Phanerozoic, South Australian Geological Survey Bulletin, 54

Elliott L.K, 2002. The sedimentary as evidence for the evolution of topography in the northern Flinders Ranges, South Australia. BSc(Hons) thesis, University of Melbourne.

Harper, K.L, 2002, Geologic and geomorphological applications of ASTER satellite imagery in the northern Flinders Ranges, South Australia. BSc(Hons) thesis, University of Melbourne.

Petts A, 2002. A morphotectonic study of the Paralana Escarpment and Yudnamutana gorge, northern Flinders Ranges. BSc(Hons) thesis, University of Melbourne.

Love D.N, Preiss W.V and Belperio A,P, 1995. Seismicity, neotectonics and earthquake risk.In: Drexel J.F & Preiss W.V (eds), The Geology of South Australia, Volume 2, The Phanerozoic, South Australian Geological Survey Bulletin, 54, 171-202.

Quigley, 2006, PhD Thesis, University of Melbourne.

Quigley, M., Cupper, M., Sandiford, M., 2006, Quaternary faults of southern Australia: palaeoseismicity, slip rates and origin, Australian Journal of Earth Sciences, 53, 285-301.

Quigley, M., Sandiford, M., Fifield, K., Alimanovic A., 2007a, Bedrock erosion and relief production in the northern Flinders Ranges, Australia. Earth Surface Processes and Landforms, 32, 929-944, doi: 10.1002/esp.1459

Quigley, M., Sandiford, M., Alimanovic, A., Fifield, L.K., 2007b, Landscape responses to intraplate deformation in the Flinders Ranges, South Australia: quantitative constraints from 10Be abundances, Earth and Planetary Science Letters, 261,120-133, doi:10.1016/j.epsl.2007.06.020.

Quigley, M., Sandiford, M., Cupper, M., 2007c, Distinguishing tectonic from climatic controls on range-front sedimentation, Flinders Ranges, South Australia. Basin Research, 19, 491–505, doi: 10.1111/j.1365-2117.2007.00336.x

Sandiford, M., 2003, Neotectonics of southeastern Australia: linking the Quaternary faulting record with seismicity and in situ stress, eds Hillis, R.R. Muller, D., Evolution and dynamics of the Australian Plate, Geological Society of Australia, Special Publication, 22, 101-113.

Teasdale, J., 1992, BSc(Hons) thesis, University of Adelaide.

Appendix - Fault geometry data.

Poontana fault
x y
139.596 -30.114
139.592 -30.137
139.590 -30.150
139.588 -30.183
139.589 -30.214
139.591 -30.230
139.592 -30.247

Wooltana fault
x y
139.536 -30.244
139.532 -30.278
139.524 -30.293
139.512 -30.307
139.497 -30.325
139.472 -30.350
(Wooltana Range Front segment)
139.447 -30.376
139.429 -30.401
139.417 -30.418
139.413 -30.425

Paralana fault
x y
139.491 -30.117
139.483 -30.134
139.478 -30.145
139.468 -30.159
139.457 -30.171
139.438 -30.187
139.405 -30.215
139.387 -30.231

Buxton Fault
x y
139.446 -30.200
139.436 -30.221
139.427 -30.243
139.417 -30.274

Adams Fault
x y
139.537 -30.122
139.549 -30.113
139.564 -30.096

139.573 -30.084

4 mile fault

x y
139.481 -30.142
139.499 -30.131
139.512 -30.119
139.529 -30.102

Parabarana Fault

x y
139.642 -30.052
139.625 -30.071
139.613 -30.086
139.604 -30.096

ATTACHMENT 2: Earthquakes within 80 km of Four Mile.

Srce	Time		Lon E	Lat S	Depth		Mag	dist	PGA	MMI	Location
ADE	1993-06-24	1302	139.5	30.1	11		ML 1.6	7	124.0	2	Arkaroola
ADE	1998-10-13	1009	139.4	30.2	12		ML 2.0	7	164.1	2	Arkaroola
ADE	1990-02-10	2209	139.5	30.2	3		ML 1.5	8	142.7	2	Arkaroola
ADE	2004-01-19	0754	139.4	30.2	10		ML 1.5	8	120.0	2	Arkaroola
ADE	1987-02-01	2209	139.6	30.1	33		ML 1.6	9	45.3	1	Paralana
ADE	1988-02-10	2000	139.4	30.2	0		ML 1.8	10	169.6	2	Arkaroola
ADE	1990-02-11	0937	139.5	30.3	7		ML 2.3	12	217.2	3	Arkaroola
ADE	1989-01-06	1305	139.6	30.2	2	G	ML 2.1	13	191.0	3	Arkaroola
ADE	1993-08-15	2310	139.4	30.1	9		ML 1.4	15	87.1	1	Arkaroola
ADE	1982-12-22	1645	139.6	30.1	0		ML 1.7	16	120.3	2	Mt Fitton
ADE	1979-02-22	0925	139.5	30.4	17		ML 2.3	21	114.9	2	Arkaroola
ADE	1987-07-12	0119	139.3	30.2	5		ML 2.0	22	108.7	2	Arkaroola
ADE	1984-09-22	0052	139.3	30.2	1		ML 2.6	24	161.7	3	Umberatana
ADE	1983-06-15	2314	139.3	30.1	11		ML 2.3	26	105.4	2	Mt Freeling
ADE	1983-06-16	0126	139.2	30.1	20		ML 1.9	28	57.8	1	Mt Freeling
ADE	2005-12-30	0129	139.4	29.9	4		ML 1.4	28	50.6	1	Mt Fitton
ADE	1986-12-16	0712	139.2	30.1	0		ML 2.0	28	82.6	2	Umberatana
ADE	1994-05-22	1935	139.6	30.4	12		ML 1.5	30	46.4	1	Balcanoona HS
ADE	2003-12-27	0155	139.3	30.4	4		ML 1.6	30	54.3	1	Arkaroola
ADE	1971-11-05	1611	139.8	30.3	7		ML 3.7	31	278.1	4	Paralana
ADE	1987-07-16	0628	139.2	30.2	29		ML 2.0	33	42.9	1	Umberatana HS
EIDC	1996-11-09	1126	139.1	30.1	0		ML 2.8	35	115.0	2	Umberatana
ADE	1982-04-28	1141	139.3	30.5	0		ML 1.7	36	46.7	1	Arkaroola
ADE	1972-03-26	1158	139.5	29.9	9		ML 1.7	36	44.6	1	Umberatana
ADE	1988-03-18	0420	139.3	30.5	10		ML 1.5	39	32.5	0	Balcanoona HS
ADE	2005-10-28	0105	139.1	30.0	10		ML 2.4	44	55.5	1	Mt Freeling
ADE	1990-07-19	0550	139.0	30.2	4		ML 1.9	44	38.4	1	Umberatana
ADE	1982-08-09	0852	139.2	30.5	9		ML 2.2	45	47.1	1	Balcanoona HS
ADE	1989-06-15	1649	139.0	30.2	11		ML 1.9	48	33.0	0	Umberatana
ADE	2004-09-21	0550	139.4	30.6	9		ML 1.4	48	22.4	-0	Wertaloona HS
ADE	1988-08-12	1336	139.2	30.5	8		ML 1.2	48	19.0	-1	Balcanoona HS
ADE	1992-06-23	0810	139.6	30.6	1		ML 1.6	48	26.6	0	Lake Frome
ADE	1989-07-24	2353	139.2	30.5	21		ML 1.4	48	19.5	-0	Hawker Hill
ADE	1990-07-27	1016	139.0	30.0	12		ML 1.5	49	22.4	-0	The Twins
ADE	1969-07-20	1747	139.3	30.6	38		ML 2.1	50	24.9	0	Wertaloona HS
ADE	1982-11-01	0748	139.1	30.4	2		ML 1.3	50	19.4	-1	Gammon Ranges
ADE	2005-11-14	1403	139.1	30.5	9		ML 2.3	50	41.7	1	Gammon Ranges
ADE	1999-10-17	1311	139.1	30.4	12		ML 2.6	50	51.9	1	Arkaroola
ADE	1992-07-26	0257	139.1	30.5	9		ML 1.3	50	18.7	-1	Hawker Hill
ADE	2002-09-07	1214	139.0	30.2	15		ML 1.9	51	28.5	0	Arkaroola
ADE	1994-10-06	0403	139.0	30.1	7		ML 2.1	51	34.9	1	Arkaroola
ADE	1975-08-29	0923	139.4	30.6	38		ML 1.9	53	19.8	-0	Balcanoona HS
ADE	2005-05-02	1652	139.0	30.3	14		ML 1.7	54	22.0	-0	Umberatana HS
ADE	2003-06-26	0951	139.0	30.4	11		ML 1.6	55	20.0	-0	Arkaroola
ADE	1987-03-09	0207	138.9	30.3	19		ML 1.7	56	19.9	-0	Arkaroola
ADE	1988-04-09	0626	139.2	30.6	6		ML 1.5	57	17.9	-1	Wertaloona HS
ADE	2005-07-22	0940	139.2	30.6	20		ML 2.4	58	32.8	1	Wertaloona HS
ADE	1980-04-26	1751	139.1	30.6	1		ML 1.5	58	17.6	-1	Nepabunna
ADE	1995-05-11	0008	139.3	30.7	5		ML 2.4	58	35.6	1	Wertaloona HS

ADE	1997-10-19	1439	139.2	30.6	19		ML 1.8	59	19.9	-0	Arkaroola
ADE	2004-01-22	1938	138.9	30.1	8		ML 1.6	60	17.8	-0	MtLyndhurst HS
ADE	1978-01-13	0042	139.0	30.5	0		ML 2.9	61	49.0	1	Nepabunna
ADE	1993-11-20	1234	138.8	30.2	11		ML 1.6	64	15.6	-1	MtLyndhurst HS
ADE	1984-12-16	0521	139.7	30.8	16		ML 1.1	66	9.5	-2	Lake Frome
ADE	1981-09-10	1748	139.4	30.8	5		ML 2.3	67	25.9	0	Lake Frome
ADE	2007-01-30	2138	138.8	30.2	17		ML 1.3	67	10.9	-1	Leigh Creek
ADE	2005-05-14	2139	138.8	30.4	9		ML 2.4	68	27.0	0	Nepabunna
ADE	2007-01-30	2136	138.8	30.1	19		ML 1.3	68	10.6	-1	Leigh Creek
ADE	1988-08-03	0739	138.9	29.8	13		ML 2.8	68	36.3	1	Murnpeowie HS
ADE	1995-07-19	0629	138.8	30.2	9		ML 1.5	69	12.7	-1	Lyndhurst
ADE	1989-12-05	1920	139.4	30.8	11		ML 1.7	69	14.6	-1	Arkaroola
ADE	1984-12-16	0501	139.8	30.7	31		ML 1.4	69	9.9	-1	Lake Frome
ADE	1985-04-18	0705	138.9	30.6	1		ML 1.2	69	10.0	-1	Nepabunna
ADE	1996-09-02	0925	139.0	30.6	10		ML 1.7	70	14.6	-1	Beltana
ADE	1994-07-08	1840	138.9	30.6	14		ML 3.3	70	50.9	2	Nepabunna
ADE	2002-09-25	0251	139.3	29.6	4		ML 2.1	70	20.0	-0	Leigh Creek
ADE	2005-03-04	0038	139.7	30.8	7		ML 3.1	70	44.2	1	Lake Frome
ADE	1995-02-08	1720	138.9	30.6	12		ML 1.6	70	13.1	-1	Nepabunna
ADE	1987-06-09	1458	138.8	30.1	20		ML 2.0	71	17.1	-0	Lyndhurst
ADE	1981-02-08	1947	139.2	30.8	2		ML 1.7	71	14.3	-1	Mulga View HS
ADE	1986-10-15	0330	139.6	30.8	11		ML 1.6	72	12.6	-1	Lake Frome
ADE	1978-08-16	1606	139.3	30.8	31		ML 1.3	73	8.4	-2	Arrowie HS
ADE	1981-04-15	0703	139.3	30.8	11		MD 2.6	73	27.3	1	Balcanoona
ADE	1981-04-15	0753	139.3	30.8	11		ML 2.6	73	27.3	1	Lake Frome
ADE	1980-05-13	0149	139.1	30.8	35		ML 2.6	73	23.0	0	Mulga View HS
ADE	1989-10-13	1646	139.2	30.8	5		ML 1.0	74	7.6	-2	Arkaroola
ADE	1964-08-16	1559	139.1	29.6	1		ML 2.3	75	20.9	0	Murnpeowie HS
ADE	1986-09-09	1754	138.7	30.3	34		ML 2.7	76	23.7	0	Leigh Creek
ADE	1987-04-23	1154	139.0	30.7	25		ML 1.4	76	9.1	-1	Nepabunna
ADE	1990-04-11	1300	138.8	29.9	10	N	ML 2.3	76	20.1	0	Umberatana
ADE	1984-08-21	1513	139.3	30.8	6		ML 2.0	76	16.0	-0	Lake Frome
ADE	1990-08-21	1106	138.8	30.5	6		ML 1.4	76	9.8	-1	Leigh Creek
ADE	1999-12-14	2150	139.1	30.8	11		ML 1.8	76	13.3	-1	Leigh Creek
ADE	1981-10-01	1717	138.7	30.2	0		ML 2.6	77	25.4	0	Lyndhurst
ADE	1990-04-09	1846	138.7	30.0	17		ML 2.4	77	20.5	0	Mt Lyall
ADE	1987-06-15	1036	138.7	30.4	11		ML 1.7	77	12.0	-1	Leigh Creek
ADE	1986-10-26	1639	138.7	30.4	24		ML 1.6	78	10.3	-1	Leigh Creek
ADE	1983-12-29	2356	139.3	30.9	4		ML 1.6	78	11.1	-1	Beltana
ISC	2005-03-03	1056	139.1	30.8	10		ML 4.0	78	75.0	3	Mulga View HS
ADE	1987-09-16	1838	138.9	30.7	0		ML 1.5	78	10.3	-1	Nepabunna
ADE	1979-06-03	1414	139.4	30.9	7		ML 1.5	78	10.1	-1	Mt Chambers
ADE	2006-07-12	0809	139.2	29.5	22		ML 1.7	79	10.9	-1	Leigh Creek
ADE	2004-06-19	0917	138.7	30.0	13		ML 1.6	79	10.5	-1	Leigh Creek
ADE	1969-03-04	0419	139.0	30.7	2		ML 3.4	80	44.9	2	Nepabunna
ADE	1986-04-02	0635	138.7	30.4	16		ML 1.2	80	7.4	-2	Leigh Creek
ADE	1986-09-10	0141	138.7	30.2	30		ML 1.9	80	11.8	-1	Mt Lyndhurst

ATTACHMENT 3. Risk Frontiers Distributed Earthquake Source Model for Australia

Lisa Hall, Felipe Dimer and Paul Somerville
Risk Frontiers, Macquarie University, North Ryde, NSW 2109, Australia
September 28, 2007

SUMMARY

A spatially distributed earthquake source model was derived by Hall et al. (2007) from the spatial smoothing of historical seismicity using the earthquake catalogue described by Leonard (2007). This approach is similar to that of Cuthbertson (2006) and to the main approach used to describe the seismic potential of the eastern United States in the U.S. National Probabilistic Seismic Hazard Maps (Frankel et al., 2007). It is intended that this model complement other models, such as Brown and Gibson (2004) and Ninis and Gibson (2006), which use geological criteria to identify zones of uniform seismic potential, and Clark (2006), which uses neotectonic data. The spatial smoothing approach has the advantages of simplicity and of avoiding uncertainty in the geological definitions of zones, but has the disadvantage of not making use of potentially informative geological data. The spatially distributed earthquake source model is in the form of a-values and b-values on a 10 km x 10 km grid throughout Australia.

A3.1. INTRODUCTION

A spatially distributed earthquake source model was derived from the spatial smoothing of historical seismicity using the earthquake catalogue described by Leonard (2007), illustrated in Figure A3.1. It contains four regions which have relatively high levels of seismic activity and catalogue completeness compared with the rest of Australia. These four regions are:

- Southeastern Australia - SEA
- Southwestern Australia – SWA
- South Australia – SA
- Northwestern Australia – NWA

The remaining area is referred to as the Rest of Australia (RA). The catalogue completeness, listed in Table A3.1, is taken from Leonard (2007) except that for SWA, we assumed completeness beginning in 1940, not 1880. There are no events in the SWA catalogue before 1940. Although it is thought that events larger than magnitude 5 should have been detected in this region since about the turn of the century, we have conservatively chosen a completeness interval starting in 1940.

Table A3.1. Completeness of the Australian Earthquake Catalogue

	>3	>3.5	>4	>4.5	>5	>5.5	>6
SEA	1960		1955		1880		1880
SA	1970			1880	1880		1880
SWA	1960			1940	1940		1940
NWA	1980		1965			1910	1910
RA	1970				1960		1910

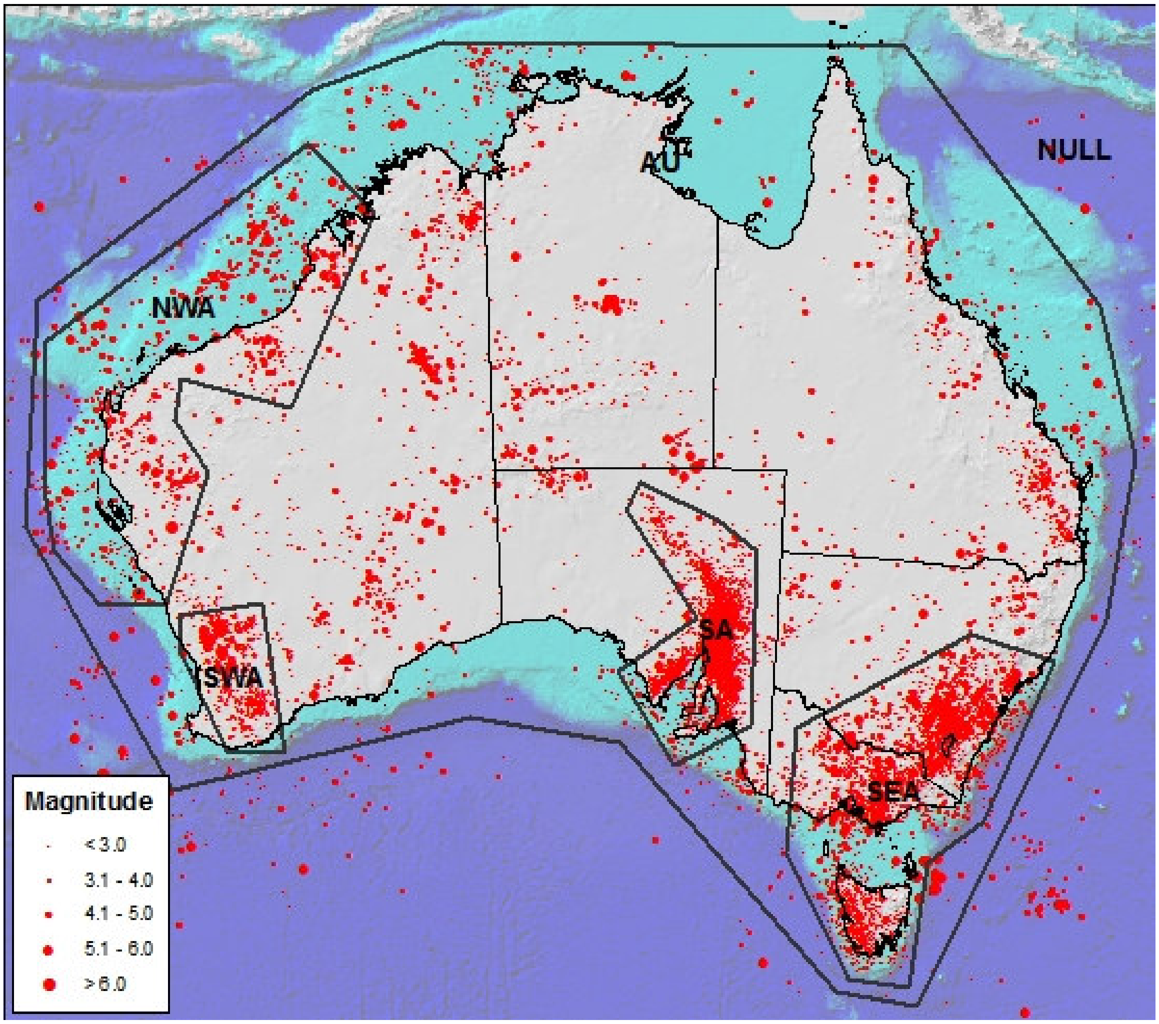

Figure A3.1: Earthquake catalogue and seismic source regions. Source: Leonard (2007).

A3.2. METHOD

The a-value grids for each region were derived from the smoothed spatial distribution of seismicity, using the b-value for that region and the number of earthquakes greater than or equal to a certain magnitude within each grid cell. We used three lower magnitude cutoff values: M3, M4 and M5, and averaged the results. We calculated separate a-value grids for each region. For each a-value grid point we calculated the number of events ≥ M0, and summed the grids for each region to give country-wide coverage of the number events ≥ M0. Kernel density algorithms were used to calculate smoothed seismicity density for each input data set. In regions with longer completeness intervals and hence higher densities of events (SEA, SWA, SA and NWA), a correlation distance of 100 km was applied. The sparse historical seismicity in the rest of Australia required greater smoothing. In this region, a seismic density grid was created by averaging smoothed grids calculated using correlation distances of 100, 200 and 300km.

The Gutenberg-Richter cumulative magnitude – frequency relation is given by:

$\mathrm{Log}_{10}N = a - bM$

where N is the number of earthquakes with magnitude equal to or larger than M. The spatially distributed earthquake source model developed in this study is provided in the form of a-values (for 100 years) and b-values on a 10 km x 10 km grid throughout Australia. The map projection used is GDA 1994, zone 53. The grid has 420 rows and 510 columns. We assume that the maximum earthquake magnitude of the distributed earthquake source is magnitude 7.5 throughout Australia. The procedure used to generate these grids of a-values and b-values is as follows.

1. Generate b-values using least squares regression for each of the following regions:
   a. Southeastern Australia - SEA
   b. Southwestern Australia – SWA
   c. South Australia - SA
   d. Northwestern Australia - NWA
   e. The Rest of Australia – Rest of AU
2. For each region calculate separate a-value grids, using the b-values determined from step 1 and appropriate completeness intervals.
3. Calculate for each a-value grid the number of events ≥ M0 (the total number of earthquakes of any magnitude) per grid cell.
4. Sum grids for each region to give a country-wide coverage of the number events ≥ M0.
5. Generate a national a-value grid

A3.3. CALCULATION OF REGIONAL b-VALUES

The b-values, listed in Table A3.2, were derived using the maximum likelihood method (Weichert, 1980), in all regions except SWA and NWA. In those two regions, we used least-squares regression, because there are inflections in recurrence curves for these regions and the maximum likelihood method is unduly sensitive to such inflections. The recurrence relations obtained using maximum likelihood and least squares are compared for each of the 5 regions in Figures A3.2 through A3.6. For SEA (Figure A3.2), the maximum likelihood estimate has a lower b-value than the least-squares estimate, and lies well above the historical data for magnitudes larger than 5.75. The discrepancy between the historical catalogue and the prediction of our model is largest for SEA, as shown in Table A3.3. The maximum likelihood estimates were made assuming a maximum magnitude of 7.5 throughout Australia.

Table A3.2. Parameters (including b values) used for each regional a-value calculation

Region	Method used *	b-value	Correlation distance (km)	Minimum Magnitudes
SEA	ML	0.82	100	M3, 4, 5
SWA	LS	0.70	100	M3, 4.5, 5
SA	ML	0.84	100	M3, 4.5, 5
NWA	LS	0.86	100	M3, 4, 5.5
Rest of AU	ML	0.82	Equally weighted average of 100, 200, 300	M3.5, 4, 5.5

* ML: maximum likelihood; LS: least squares

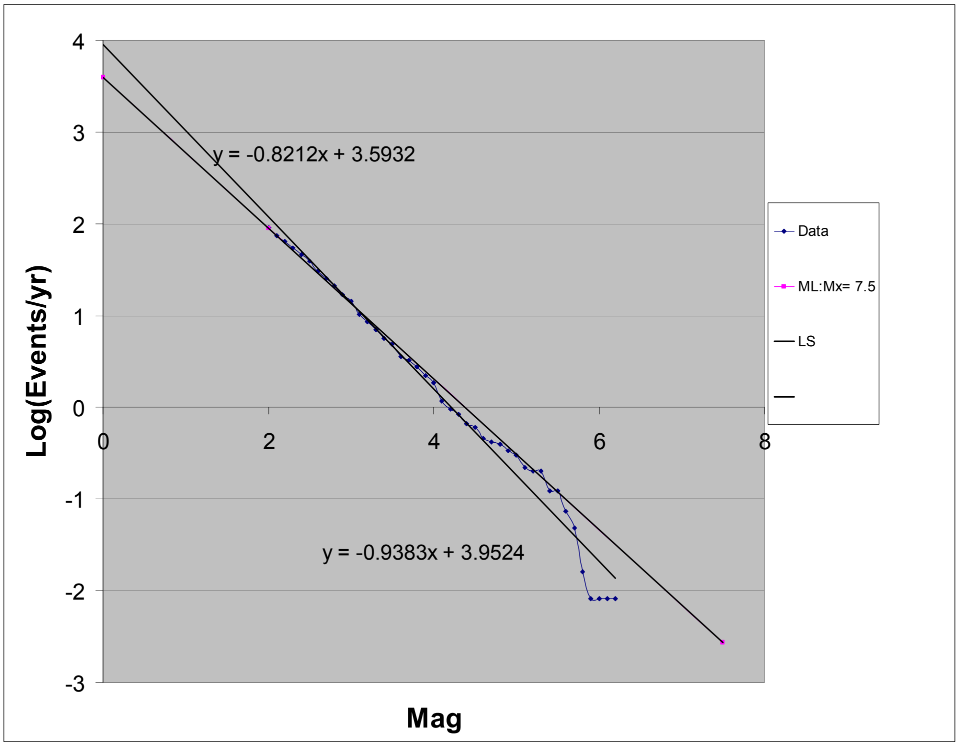

Figure A3.2. Recurrence data and recurrence relations for SEA using least squares (LS; black line) and maximum likelihood (ML; purple line).

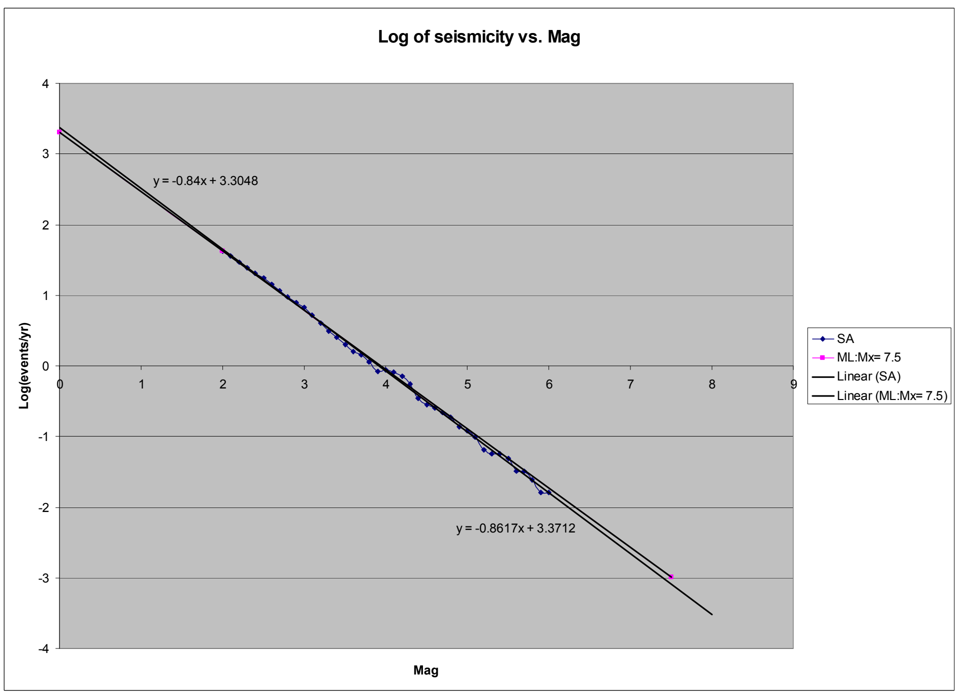

Figure A3.3. Recurrence data and recurrence relations for SA using least squares (LS; black line) and maximum likelihood (ML; purple line).

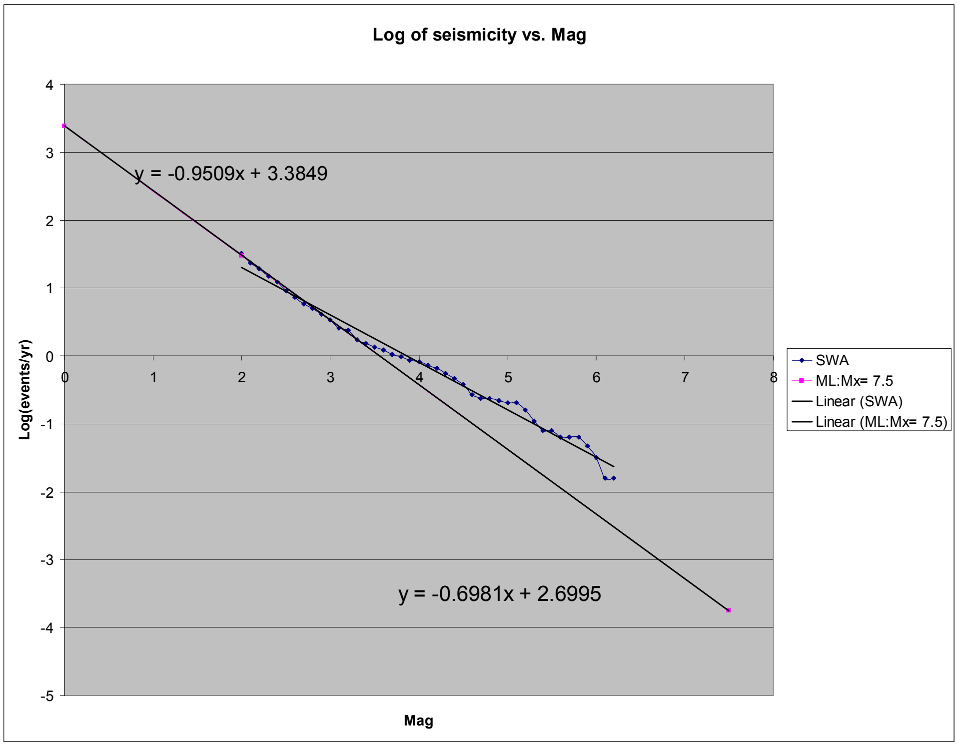

Figure A3.4. Recurrence data and recurrence relations for SWA using least squares (LS; black line) and maximum likelihood (ML; purple line).

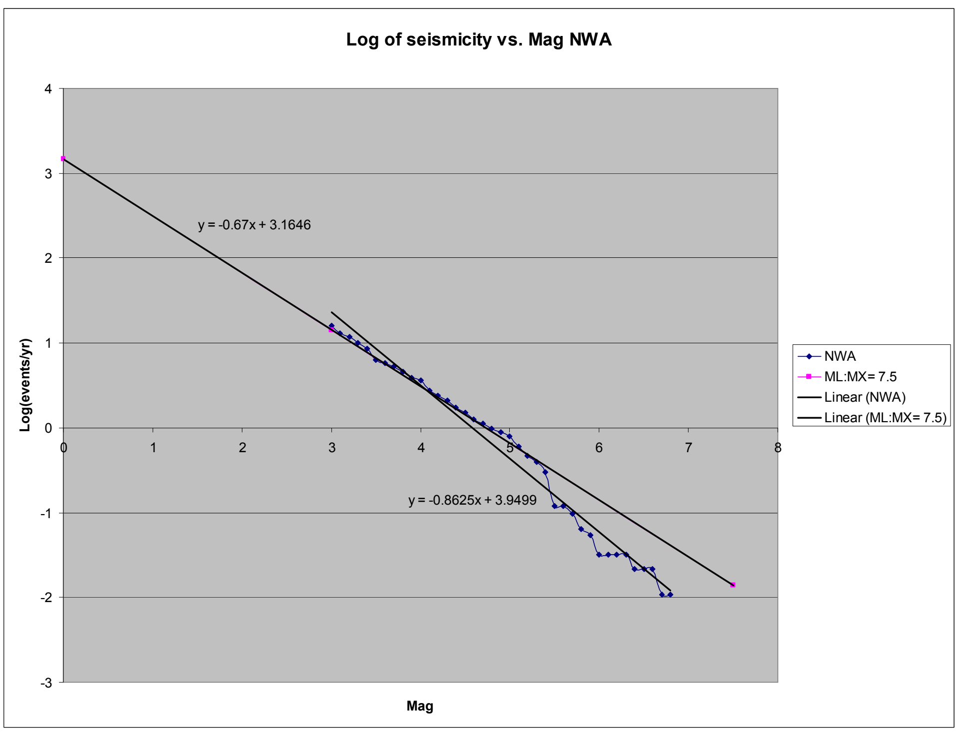

Figure A3.5. Recurrence data and recurrence relations for NWA using least squares (LS; black line) and maximum likelihood (ML; purple line).

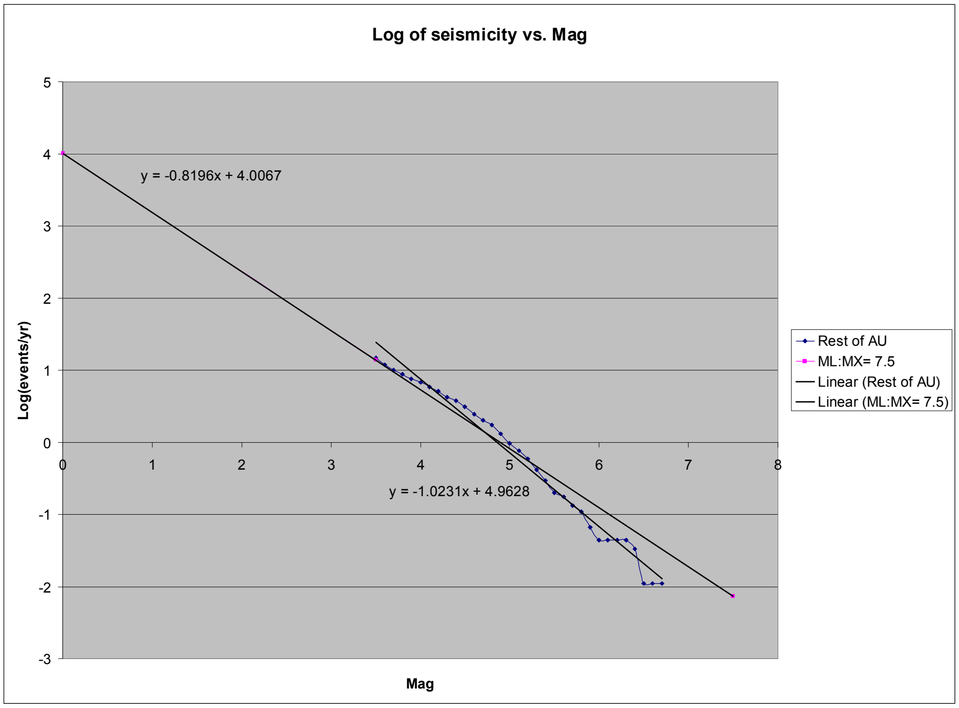

Figure A3.6. Recurrence data and recurrence relations for the Rest of AU using least squares (LS; black line) and maximum likelihood (ML; purple line).

A3.4. CALCULATION OF a-VALUE GRIDS

The a-values for each 10 x 10 km grid cell were derived from the smoothed spatial distribution of historic seismicity, using the b-values and the number of earthquakes greater or equal to a certain magnitude within each grid cell. Unless the cumulative magnitude – frequency relation shows no deviation from a straight line, the a-value calculated will depend on the minimum magnitude used. The calculation is therefore repeated using three different magnitude ranges, so an average may be calculated.

The steps involved in calculating a-value grids for each region and for each minimum magnitude are as follows:

i) Input spatial databases are created for each region containing all events greater or equal to a defined minimum magnitude within the completeness interval from Leonard (2007). For each of the four regions, three input databases are used, with minimum magnitudes of M3, M4 and M5. For the rest of AU, the catalogue is not complete down to magnitudes of M3, so minimum magnitudes of M3.5, M4 and M5 are applied

ii) Kernel density algorithms calculate smoothed seismicity density (per km^2) for each input database. In regions with longer completeness intervals and hence higher densities of events (SEA, SWA, SA and NWA) a correlation distance of 100 km is applied. The rest of the country requires greater smoothing due to the sparse data distribution. In this region, a seismic density grid is created by averaging smoothed grids calculated using correlation distances of 100, 200 and 300km. Smoothing uses a quadratic kernel function.

iii) Within a region, kernel density maps for each minimum magnitude are averaged and divided by the completeness interval, to give event rates of Mx and greater. Numbers are adjusted to give rate per 100 years, per 100 km^2 grid cell.

iv) The number of events ≥ Mx and the b-values are used to calculate the a-value for each grid cell.

v) a-values are then converted to a grid of the number of events of M0 and greater.

The parameters used in this process are given in Table A3.2. These include the regional b-value, the correlation distance used in spatial smoothing, the magnitudes that were separately smoothed and combined, and the completeness intervals.

To create the final a-value grid for each region, the a-values calculated from the different magnitude ranges are averaged as follows:

i) Input grids calculated for different minimum magnitudes give the number of events of M0 and greater (over 100 years, in each grid cell - an area of 100km^2).

ii) Where cells have no data, cells are populated with a rate of 0.

iii) Event rate grids are averaged using equal weights

iv) An a-value is calculated from the averaged event rate grid.

We averaged the grids of event frequency ≥ M0 (i.e. 10^a), rather than a-value. Averaging a-values gives a closer answer to least squares regression, but does not deal with regions of no seismicity. Averaging event rates gives a slightly less accurate result but accounts for areas of no historical activity.

The event frequency grids for each region are summed to produce a country-wide coverage of the number events ≥ M0. This is converted to a-value using the national b-value grid.

A3.5. DISCUSSION

The gridded "a" values are shown at the top of Figure A3.7, and the predicted number of earthquakes of magnitude equal to or larger than 5 predicted by our model is shown at the bottom of Figure A3.7. There is fairly good agreement between the "a" values and "b" values of our model and that of Leonard (2007), but the latter model has a lower b-value in Southwestern Australia than our model (0.58 compared with 0.70). The distributed earthquake source model is compared with the historical earthquake catalogue of Leonard (2007) in Table A3.3. This table compares predicted rates of earthquakes in different magnitude ranges with historical values in each of the regions. The agreement overall is good for magnitudes up to 5, but there is a tendency for our model to overpredict the numbers of recorded earthquakes having magnitudes of 6.0 and larger.

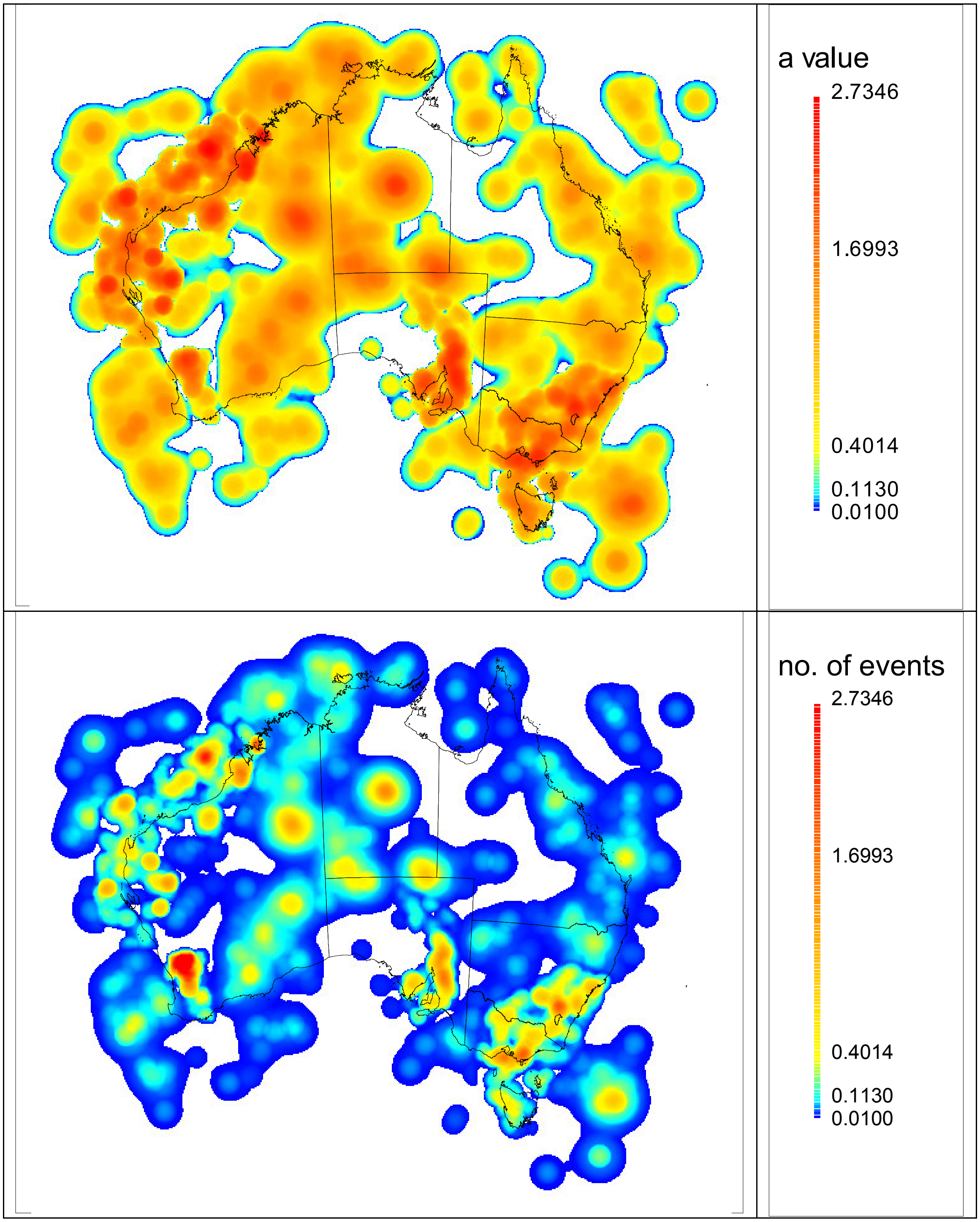

Figure A3.7. Top: Grid of "a" values, normalised to 100 years and 100 square km. Bottom: Grid of number of events of M>5 per 500 years per 10,000 square km.

Table A3.3: Comparison of source model and earthquake catalogue event rates

	SEA				SWA				SA			
	≥M3	**≥M4**	**≥M5**	**≥M6**	**≥M3**	**≥M4.5**	**≥M5**	**≥M6**	**≥M3**	**≥M4.5**	**≥M5**	**≥M6**
Catalogue Event Rate per 100 yr	**1393**	**180**	**30**	**0.8**	**334**	**32**	**20**	**3.1**	**662**	**28**	**10**	**0.8**
Model Event Rate per 100 yr	**1264**	**191**	**29**	**4.3**	**390**	**35**	**15**	**3.0**	**557**	**31**	**12**	**1.6**
% Diff	-9%	6%	-3%	387%	13%	3%	-25%	3%	-15%	10%	20%	100%

	NWA				Rest of AU			All AU		
	≥M3	**≥M4**	**≥M5.5**	**≥M6**	**≥M4**	**≥M5**	**≥M5.5**	**≥M4**	**≥M5**	**≥M6**
Catalogue Event Rate per 100 yr	**1554**	**354**	**12**	**3.2**	**574**	**77**	**19**	1313	219	11
Model Event Rate per 100 yr	**1774**	**243**	**12**	**4.6**	**597**	**90**	**35**	**1189**	**179**	**27**
% Diff	14%	-31%	0%	43%	4%	29%	100%	-9%	-18%	147%

A3.6. CONCLUSIONS

A spatially distributed earthquake source model was derived from the spatial smoothing of historical seismicity using the earthquake catalogue described by Leonard (2007). It is intended that this model complement other models, such as Brown and Gibson (2004) and Ninis and Gibson (2006), which use geological criteria to identify zones of uniform seismic potential, and Clark (2006), which uses neotectonic data. In the approaches developed by Brown and Gibson (2004) and Ninis and Gibson (2006), some of the seismicity was associated with specific faults, but this has not yet been done in the present model. The spatial smoothing approach has the advantages of simplicity and of avoiding uncertainty in the geological definitions of zones, but has the disadvantage of not making use of potentially informative geological data.

A3.7. ACKNOWLEDGMENTS

The authors are grateful to Mark Leonard for permission to publish Figure A3.1.

A3.8. REFERENCES

Brown, A. and G. Gibson (2004). A multi-tiered earthquake hazard model for Australia. *Tectonophysics 390*, 25-43.

Clark, D. (2006). A seismic source zone model based on neotectonics data. *Earthquake Engineering in Australia,* Canberra 24-26 November.

Cuthbertson, R. (2006). Automatic calculation of seismicity rates in eastern Queensland. *AEES Conference, Earthquake Engineering in Australia,* Canberra, 24-26 November.

Frankel, A., C. Mueller, T. Barnhard, D. Perkins, E. Leyendecker, N. Dickman, S. Hanson and M. Hopper (1996). National Seismic Hazard Maps, June 1996. *U.S. Geological Survey Open File Report* 96-532.

Gaull, B.A., Michael-Leiba M. and Rynn J.M.W. 1990. Probabilistic earthquake risk maps of Australia. *Australian Journal of Earth Sciences* **37**, 169-187.

Hall, L., F. Dimer and P.Somerville (2007). A Spatially Distributed Earthquake Source Model for Australia. Proceedings of the 2007 Annual Meeting of the Australian Earthquake Engineering Society.

Leonard, M. (2007). One hundred years of earthquake recording in Australia. *Bull. Seism. Soc. Am.*, in press.

Leonard, M. and D. Clark (2006). Reconciling neotectonic and seismic recurrence rates in SW WA. *Earthquake Engineering in Australia*, Canberra 24-26 November.

Ninis, D. and G. Gibson (2006). Developing a seismotectonic model using neotectonic setting and historical seismicity – application to central NSW. *AEES Conference, Earthquake Engineering in Australia,* Canberra, 24-26 November.

Weichert, D. (1980). Estimation of the earthquake recurrence parameters for unequal observation periods for different magnitudes. *Bull. Seism. Soc. Am*. 70, 1337-1346.